

Molecular Probes for Tracking Lipid Droplet Membrane Dynamics



Open Access This file is licensed under a Creative Commons Attribution 4.0 International License, which permits use, sharing, adaptation, distribution and reproduction in any medium or format, as long as you give appropriate credit to the original author(s) and the source, provide a link to the Creative Commons license, and indicate if changes were made. In the cases where the authors are anonymous, such as is the case for the reports of anonymous peer reviewers, author attribution should be to 'Anonymous Referee' followed by a clear attribution to the source work. The images or other third party material in this file are included in the article's Creative Commons license, unless indicated otherwise in a credit line to the material. If material is not included in the article's Creative Commons license and your intended use is not permitted by statutory regulation or exceeds the permitted use, you will need to obtain permission directly from the copyright holder. To view a copy of this license, visit <http://creativecommons.org/licenses/by/4.0/>.

Editorial note: Parts of this Peer Review File have been redacted as indicated to remove third-party material where no permission to publish could be obtained.

REVIEWER COMMENTS

Reviewer #1 (Remarks to the Author):

In this study, the authors introduced a novel molecular probe for tracking lipid droplet (LD) membrane dynamics. The utilization of the LDM pro-probe allows for precise labeling of the LD membrane in live cells super-resolution imaging, providing valuable insights into the dynamic mechanisms of LD membrane contacts and adhesion parameters. They also applied this probe in liver cancer cells, which led to the discovery of enhanced LD-mitochondria interactions during energy stress, highlighting its potential in studying metabolic diseases. Overall, this work demonstrates the utility of the LDM probe in advancing our understanding of LD membrane biology and developing a new tool for investigating regulatory mechanisms and biological functions associated with LD-related metabolic diseases. The probe development is very novel, most of the conclusions are solid and well supported by their data, and the paper is very well written. The brand new LD membrane tool proposed in this manuscript will broaden the scope of future LD cell biological research. This comprehensive study involving chemists, biophysicists, and membrane biologists fits the scope of Nat. Commun well. Therefore, I strongly suggest publication after a minor revision.

Comment 1: The cytotoxicity of LDM-OH needs to be added, similar to LDM for 24 hours in HeLa and HepG2 cells.

Comment 2: In Figure 5a, the author claims that the viscosity and quantity of lipid droplets decrease under starvation, which needs to be supported by the changes in triglyceride content of lipid droplets under starvation.

Comment 3: In the text description corresponding to Fig. 2a, 405 nm and 561 nm should be UV absorption peaks rather than fluorescence intensity. Some italicized text needs to be paid attention to, such as *n*, *P*, etc.

Comment 4: The parameter "colocalization coefficient" needs to be thoroughly explained either in the results section or the experimental section. It is crucial to provide a clear definition of how it is defined, measured, and quantified.

Comment 5: In Fig. 1, the schematic diagram of the chemical strategy to selectively label LD membranes, the middle part of Figure 1b is blurry, it is recommended to replace it with a clearer image.

Comment 6: In Figures 4a, FI1, FI2, and FI3 correspond to values and coordinates that are similar, which can easily lead to misunderstandings. Please use a different expression for coordinates.

Comment 7: In Figures 5a and j, the text annotation positions should be uniformly located in the upper right corner with clear colors.

Reviewer #3 (Remarks to the Author):

This work from Kong et al. entitled "Molecular Probes for Tracking Lipid Droplet Membrane Dynamics 1" aims at developing a probe to label protein coats on LD specifically, by developing a new probe they called LDM.

The synthesis and characterization of LDM, as shown in the first two figures, are well-executed. However, the subsequent cellular usage, analysis and interpretation of LDM's recruitment to the LD surface, and its role in LD interactions or adhesion with mitochondria during energy demands, raise several concerns.

Firstly, the differentiation between this approach and simply tagging proteins is unclear, except for the fact that the labeling in the author's method is non-specific. The physical and biological interpretations provided are premature and need substantial refinement. There are many other issues. I list some examples in the following.

The statement "The uneven distribution might, therefore, be due to different protein distribution patterns within different red-like ring structures, particularly at the contact site," could be explained by the simple proximity of two droplets, which increases the signal in the contact.

"This suggests that the red ring-like structures labeled by LDM may represent the LD membrane." The lipid membrane of phospholipids is not the same as the protein coat. LDs are coated with peripheral proteins whose thickness in the cytosol varies.

"Therefore, we believe that the size of the LDM-based ring is a more accurate representation of the LD size." This is not necessarily true, especially in cases where there is a thick protein coat.

"Consequently, we propose that our probe captures the real contact sites between multiple LD interactions in living cells (Fig. 3g)." This conclusion lacks sufficient convincing evidence and, again, proximity does not necessarily reflect contact sites.

"We also noticed that the fluorescence intensity of the LDM561 marker at the contact site is more than twice that of the non-contact site (Supplementary Fig. 27), suggesting that the high fluorescence intensity might be due to accumulation of labeled proteins at specific sites."

The increased intensity could merely be due to the close proximity of two fluorescent interfaces, which would double the signal irrespective of adhesion.

This referee encourages the authors to revisit the interpretations and conclusions drawn from your data and to think more about the valorization of their tool.

[Editorial note: The report of Reviewer 2 begins on the next page.]

In this paper, the authors designed a LD membrane labeling pro-probe **LDM**, which releases **LDM-OH** when it is activated by the HClO/ClO⁻ microenvironment around the lipid droplets, and **LDM-OH** can bind to the LD membrane protein to further locate **LDM** on the lipid droplet membrane, thus realizing the visualization of the ring-like LD membrane. In my opinion, the work is novel and organized well, and the results are reasonable. Thus, I recommend it for publication in *Nature Communications* after the following minor revisions:

- 1, As an important parameter of fluorescence properties, it is necessary to provide the fluorescence quantum yield of **LDM** with or without ClO⁻.
- 2, **LDM** can specifically target lipid droplets membrane, and lipid droplets are organelles with high viscosity and low polarity, so is **LDM** sensitive to viscosity or polarity? And **LDM-OH**?
- 3, The detection limit of **LDM** for ClO⁻ (6.8 μM) may be too high to detect subtle changes of ClO⁻ in cell microenvironment with high sensitivity.
- 4, The author should provide the response time between **LDM** and ClO⁻.
- 5, In the selective experiment, the author should supplement the response of **LDM** to O_2^- .
- 6, The author should give the UV-vis absorption spectra of **LDM**, **LDM-OH** and the reaction of **LDM** with ClO⁻.
- 7, It is recommended that the author change to a clearer version of **Supplementary Figure 11**.
- 8, NMR characterization should be standardized, for example, the chemical shift unit (ppm) is missing.
- 9, There are some errors in manuscript and ESI, including but not limited:
 - 1) Line 329, the author mentioned “DMSO-PBS, pH = 7.4, 1:1, v/v”, while in line 403 and 410, “DMSO-PBS, pH = 7.4, 1:99, v/v”.
 - 2) **Supplementary Figure 10** does not correspond to line 324 of the manuscript.
 - 3) Line 342, the author should confirm whether (NH₄)₂SO₄·6H₂O is (NH₄)₂Fe(SO₄)₂·6H₂O?

Response to the reviewers' comments

We thank the reviewers for their constructive criticism and for noting the importance of our study. We have revised the manuscript accordingly and all their concerns have been addressed by appropriate revision of the text. We deeply appreciate the valuable feedback from all the reviewers, which helped us further improve the manuscript. During the revision, we conducted a significant number of new experiments to address all the issues raised by the reviewers, including updated Figures 1-5 and the incorporation of 20 new supplementary figures (Fig. S2-3, S5-6, S8-9, S11, S13-16, S18, S21, S27-29, S36, S43, S45-46). All the changes are highlighted in red. Our point-by-point responses to the reviewers' comments are summarized as follows.

Reviewer #1 (Remarks to the Author):

In this study, the authors introduced a novel molecular probe for tracking lipid droplet (LD) membrane dynamics. The utilization of the LDM pro-probe allows for precise labeling of the LD membrane in live cells super-resolution imaging, providing valuable insights into the dynamic mechanisms of LD membrane contacts and quantum yield parameters. They also applied this probe in liver cancer cells, which led to the discovery of enhanced LD-mitochondria interactions during energy stress, highlighting its potential in studying metabolic diseases. Overall, this work demonstrates the utility of the LDM probe in advancing our understanding of LD membrane biology and developing a new tool for investigating regulatory mechanisms and biological functions associated with LD-related metabolic diseases. The probe development is very novel, most of the conclusions are solid and well supported by their data, and the paper is very well written. The brand new LD membrane tool proposed in this manuscript will broaden the scope of future LD cell biological research.

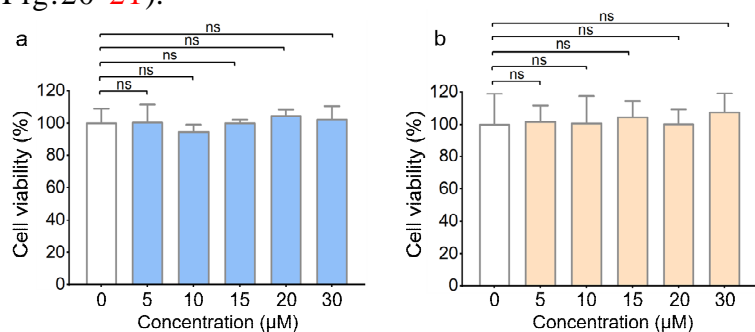
This comprehensive study involving chemists, biophysicists, and membrane biologists fits the scope of Nat. Commun well. Therefore, I strongly suggest publication after a minor revision.

We thank the reviewer for the positive note on our manuscript and valuable comments.

Comment 1: *The cytotoxicity of LDM-OH needs to be added, similar to LDM for 24 hours in HeLa and HepG2 cells.*

Response: Thanks for the comment. According to the reviewer's suggestion, we have added this assay. The result showed that the cytotoxicity of LDM-OH for 24 h in HeLa and HepG2 cells had no cytotoxicity at high concentrations. We added this result as new Supplementary Figure 21. **It reads now:**

Line 146: We first evaluated the cytotoxicity of LDM and LDM-OH on HeLa/HepG2 cell lines and found that the toxic effect of LDM on cell activity was negligible (Supplementary Fig.20-21).



New Supplementary Figure 21. The cell survival rate (%) obtained through CCK-8 measurement. HeLa (the left side) and HepG2 (the right side) cells were incubated with different concentrations of LDM-OH (0.0 µM, 5.0 µM, 10.0 µM, 20.0 µM, 30.0 µM) for 24 h.

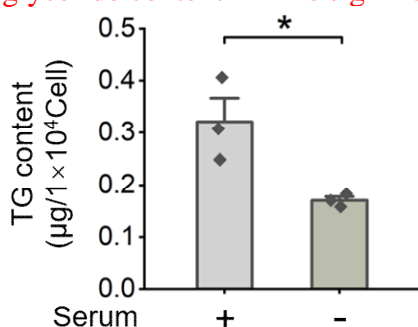
The error bar represents the standard deviation ($n=6$).

Comment 2: In Figure 5a, the author claims that the viscosity and quantity of lipid droplets decrease under starvation, which needs to be supported by the changes in triglyceride content of lipid droplets under starvation.

Response: Thank you for the reviewer's suggestion. We have added data on the changes in triglyceride content in LDs under starvation. We added this result as new Supplementary Figure 43.

It reads now:

Line 236: We found that the LD in liver cancer cells significantly decrease in a starving state, with the number and area of LD reduced by approximately 2-3 times (Fig. 5a-c) and the triglyceride content in LDs significantly decreases (Supplementary Fig.43).



New Supplementary Figure 43. Comparison of TG content in HepG2 cells under serum-fed and serum-free conditions. $n = 3$. Data are shown as mean \pm SE ($*p < 0.05$).

Comment 3: In the text description corresponding to Fig. 2a, 405 nm and 561 nm should be UV absorption peaks rather than fluorescence intensity. Some italicized text needs to be paid attention to, such as n , P , etc.

Response: Thanks to the reviewer's comments, we have corrected this accordingly. **It reads now:**

Line 115: "Additionally, we observed a decrease in absorption peak at 405 nm, suggesting that LDM responds to HClO/ClO^- to generate LDM-OH *in vitro*."

And we have rechecked the format and details in the manuscript, such as n , P , etc. The modified parts have been highlighted in red.

Comment 4: The parameter "colocalization coefficient" needs to be thoroughly explained either in the results section or the experimental section. It is crucial to provide a clear definition of how it is defined, measured, and quantified.

Response: We thank the reviewer's comment. We have already expanded this part in the method section.

It reads now:

Line 410: "In addition, Pearson correlation coefficient (PCC, the degree of overlap between two fluorescent channels, pixel-based) was analyzed for co-localization using ImageJ software equipped a colocalization analysis plugin as previously reported⁵⁴. For more information, please refer to https://imagejdocu.tudor.lu/plugin/analysis/colocalizationfinder/start#colocalization_finder."

Comment 5: In Fig. 1, the schematic diagram of the chemical strategy to selectively label LD membranes, the middle part of Figure 1b is blurry, it is recommended to replace it with a clearer image.

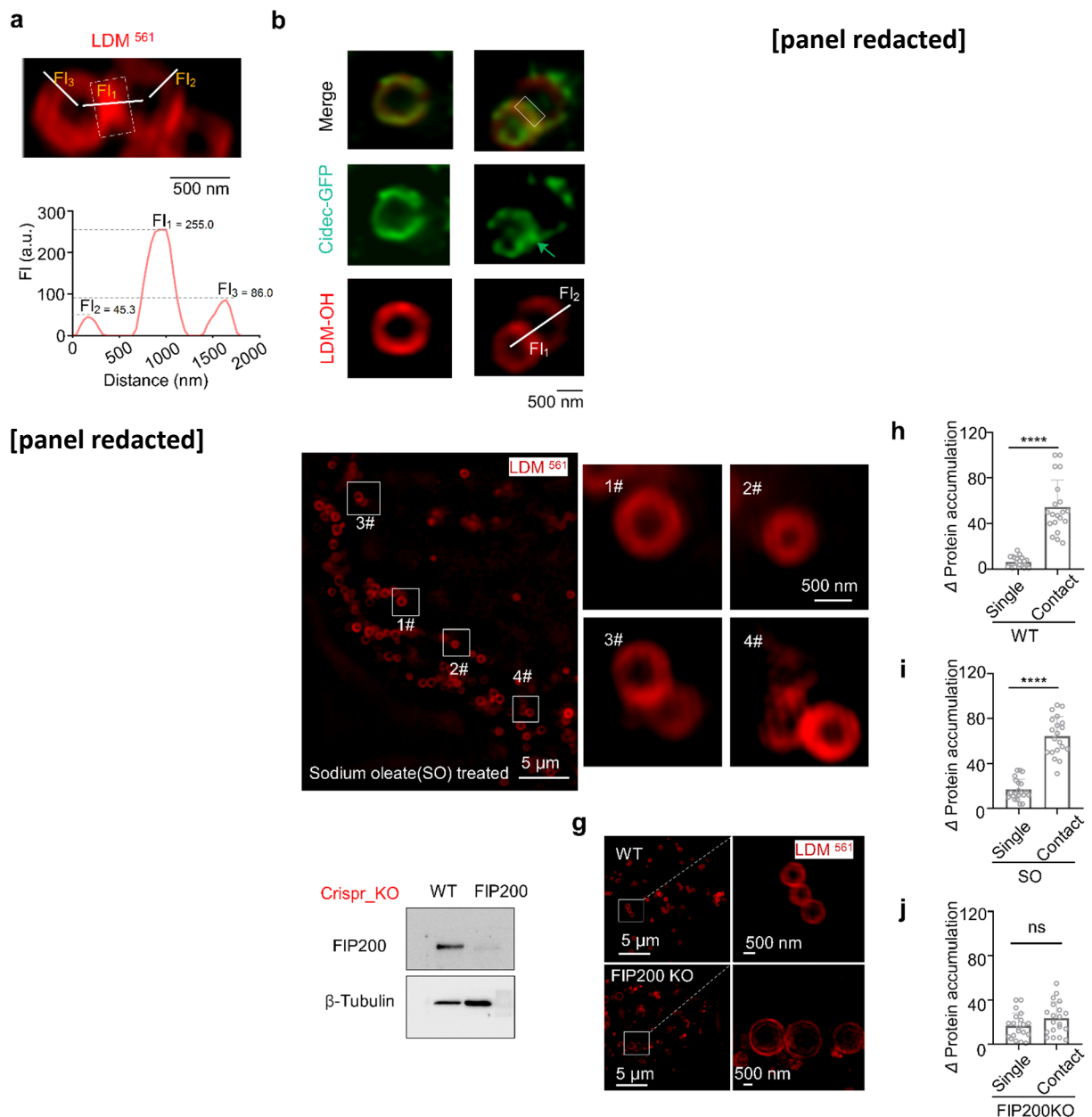
Response: We have replaced Figure 1 with a clear image: **It reads now:**

[figure redacted]

Revised Fig. 1. Schematic diagram of chemical strategy to selectively label LD membranes.

Comment 6: In Figures 4a, FI1, FI2, and FI3 correspond to values and coordinates that are similar, which can easily lead to misunderstandings. Please use a different expression for coordinates.

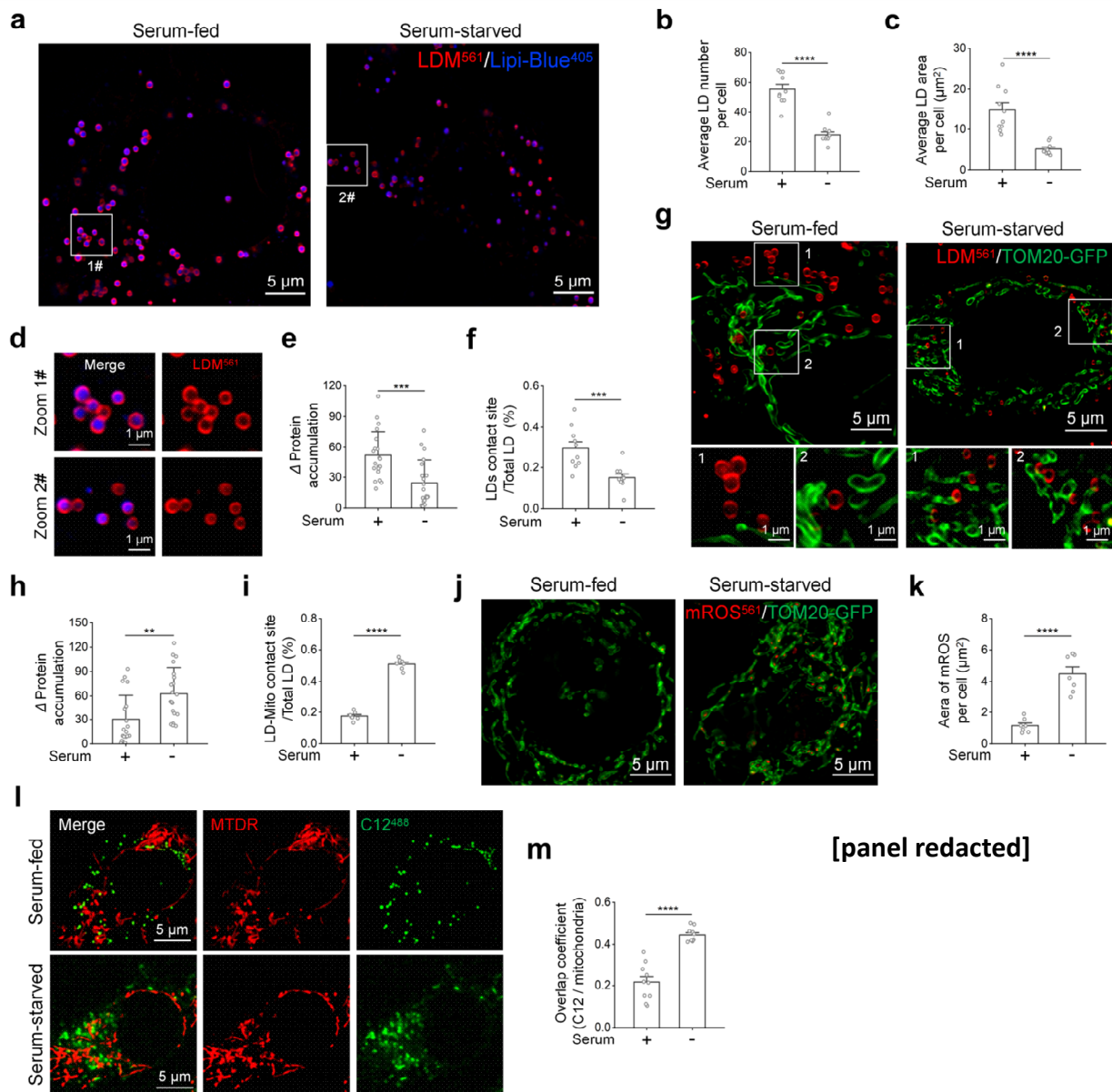
Response: Thank you for the reviewer's suggestions. We have revised and replaced Figure 4.



Revised Fig. 4. LDM fluorescence aggregation as an indicator of membrane contact protein accumulation parameters.

Comment 7: In Figures 5a and j, the text annotation positions should be uniformly located in the upper right corner with clear colors.

Response: Thank you for the reviewer's suggestions. We have revised and replaced Figure 5a and j.



Revised Fig. 5. Using LDM to track changes in LD membrane adhesion force during the period of liver cancer cell starvation.

Reviewer #2

In this paper, the authors designed a LD membrane labeling pro-probe **LDM**, which releases **LDMOH** when it is activated by the HClO/ClO^- microenvironment around the lipid droplets, and **LDMOH** can bind to the LD membrane protein to further locate **LDM** on the lipid droplet membrane, thus realizing the visualization of the ring-like LD membrane. In my opinion, the work is novel and organized well, and the results are reasonable.

Thus, I recommend it for publication in Nature Communications after the following minor revisions:

We thank the reviewer for noting the novelty of our work.

Comment 1: As an important parameter of fluorescence properties, it is necessary to provide the fluorescence quantum yield of **LDM** with or without ClO^- .

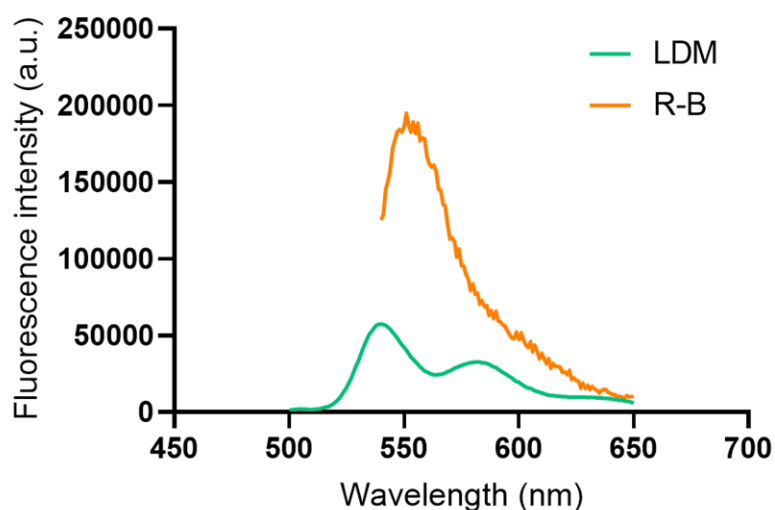
Response: In agreement with the reviewer's comment, we added the fluorescence quantum yield of **LDM** with or without ClO^- . The fluorescence quantum yield of **LDM** is calculated using the following formula: Φ_{LDM} represents the fluorescence quantum yield of **LDM**, and $\Phi_{\text{R-B}}$ is the fluorescence quantum yield of standard Rhodamine B (Rhodamine B in ethanol $\Phi = 0.82$); F_{LDM} and $F_{\text{R-B}}$ are the maximum fluorescence emission intensities when excited at 488 nm and 568 nm; A_{LDM} and $A_{\text{R-B}}$ are absorbances at fixed excitation wavelengths, with measured values of $A = 0.1$.

$$\Phi_{\text{LDM}} = \frac{\Phi_{\text{R-B}} \times F_{\text{LDM}} \times A_{\text{R-B}}}{F_{\text{R-B}} \times A_{\text{LDM}}}$$

The calculated Φ_{LDM} value is 0.23.

We add this result as new Supplementary Figure 14. **It reads now:**

Line 114: **LDM** has a fast ability to respond to ClO^- (response time < 40 min), with a fluorescence quantum yield of 0.23 (Supplementary Fig. 14).



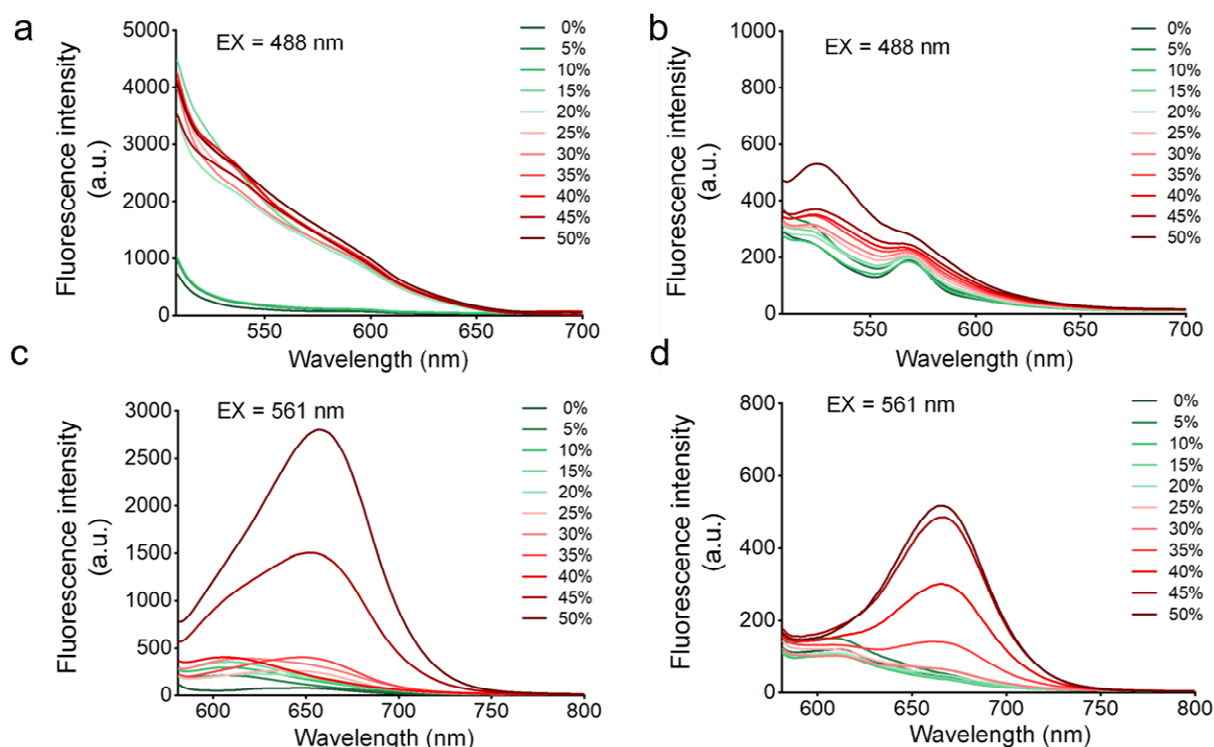
New Supplementary Figure 14. Fluorescence intensity of **LDM** and Rhodamine solutions. (UV absorption $A = 0.10$, FLS1000, **LDM** soluble in DMSO, Rhodamine soluble in methanol).

Comment 2: **LDM** can specifically target lipid droplets membrane, and lipid droplets are organelles with high viscosity and low polarity, so is **LDM** sensitive to viscosity or polarity? And **LDM-OH**?

Response: We apologize for the confusion. We have added viscosity and polarity assay for **LDM** and **LDM-OH**. Results indicate that an increase in viscosity has a non-linear

strengthening effect on the fluorescence intensity of **LDM** and **LDM-OH**. The effect of polarity on **LDM** is not significant. When the content of dioxane is 40-50%, the polarity of the solution enhances the fluorescence intensity of **LDM-OH**. We added this result as new Figure S16. **It reads now:**

Line 118: Simultaneously investigated the effects of viscosity and polarity on **LDM** and **LDM-OH**. Results indicate that an increase in viscosity has a non-linear strengthening effect on the fluorescence intensity of **LDM** and **LDM-OH**. The effect of polarity on **LDM** is not significant. When the content of dioxane is 40% -50%, the polarity of the solution enhances the fluorescence intensity of **LDM-OH** (Supplementary Figure 16).



New Supplementary Figure 16. The effects of viscosity and polarity on **LDM** and **LDM-OH**. (a) The effect of viscosity (glycerol content) on **LDM**; (b) The effect of polarity (dioxane content) on **LDM**; (c) The effect of viscosity (glycerol content) on **LDM-OH**; (d) The effect of polarity (dioxane content) on **LDM-OH**. **LDM**: $\lambda_{ex} = 488$ nm, slit: 10 nm/10 nm/700 V. **LDM-OH**: $\lambda_{ex} = 561$ nm, slit: 10 nm/10 nm/700 V.

Comment 3: The detection limit of **LDM** for ClO^- ($6.8 \mu\text{M}$) may be too high to detect subtle changes of ClO^- in cell microenvironment with high sensitivity.

Response: Thanks for the reviewer's comments, The reason for this result is due to the inconsistency of the *in vitro* and *in vivo* environments, which is difficult to mimic the *in vivo* environment *in vitro*, and this was confirmed by our examination of the *in vitro* assay lines of a recent series of ClO^- probes, such as LOD = $2.7 \mu\text{M}$ (*Chem. Commun.*, 2024, 60, 835–838); LOD = $2.16 \mu\text{M}$ (*Sensors and Actuators: B. Chemical* 347 (2021) 130620); LOD = $1.58 \mu\text{M}$ (*Adv. Mater.* 2023, 35, 2307008), Our results are similar to these. In addition, the high detection limit also provides a high degree of protection against imaging interference from within the cellular matrix, better protecting the probe from reaching the periphery of the LD. To address the reviewers' concerns, we have added a discussion of this result. **It reads now:**

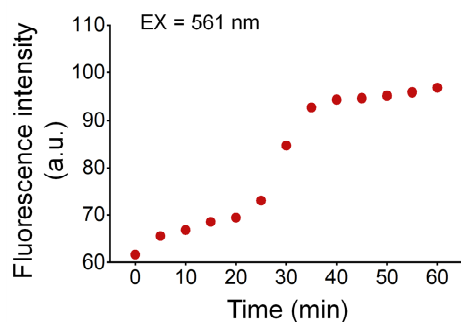
Line 110: To confirm that HClO/ClO^- triggers activation of **LDM**, we added NaClO (HClO/ClO^- donor¹⁸), which led to an increase in fluorescence intensity at 561 nm, showing a linear correlation with $R^2 = 0.98933$, and a detection limit of $6.8 \mu\text{M}$ (Fig. 2a–c,

Supplementary Fig. 12), which depends on the environment of *in vitro* simulation testing.²⁰⁻²²

Comment 4: The author should provide the response time between **LDM** and ClO^- .

Response: Thank you for underlining this deficiency. We have added an assay to check the response time between **LDM** and ClO^- . **LDM** has a fast ability to respond to ClO^- , which response time < 40 min. We add this result as new Supplementary Figure13, **it reads now:**

Line 114: **LDM** has a fast ability to respond to ClO^- (response time < 40 minutes) (Supplementary Fig. 13)...



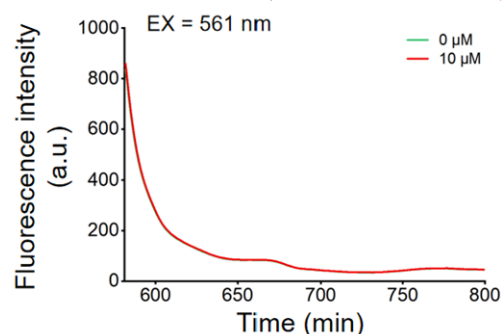
New Supplementary Figure13. The response time between **LDM** and ClO^- . **LDM** (10.0 μM) in different NaClO (100.0 μM) solution (DMSO-PBS,1:99, v/v, pH = 7.4), $\lambda_{\text{ex}} = 561\text{nm}$, slit: 5 nm/5 nm/700 V.

Comment 5: In the selective experiment, the author should supplement the response of **LDM** to $\cdot\text{O}^{2-}$.

Response: According to the reviewer's suggestion, we have added an experiment on response of **LDM** to $\cdot\text{O}^{2-}$. We add this result as new Supplementary Figure 18. **It reads now:**

Line 126: At 10.0 μM , only HClO/ClO^- triggered a fluorescence signal response centered at 665 nm, while no significant changes were observed in the presence of other ROS or biologically related species, such as H_2O_2 , $\cdot\text{OH}$, $\cdot\text{O}^{2-}$, metal ions (Fig. 2e, Supplementary Fig. 17,18), or pH changes (Fig. 2d)

Line 378: Various reactive oxygen species (ROS) and reactive nitrogen species (RNS), including NO_2^- , NO_3^- , ClO^- , H_2O_2 , $^1\text{O}_2$, $\cdot\text{OH}$, NO , t-BuOO^- , ONOO^- , and $\cdot\text{O}^{2-}$ were prepared using the following method. NO_2^- , NO_3^- and $\cdot\text{O}^{2-}$ were prepared with corresponding sodium salts NaNO_2 , NaNO_3 and KO_2 , respectively, with a final concentration of 0.01 M.



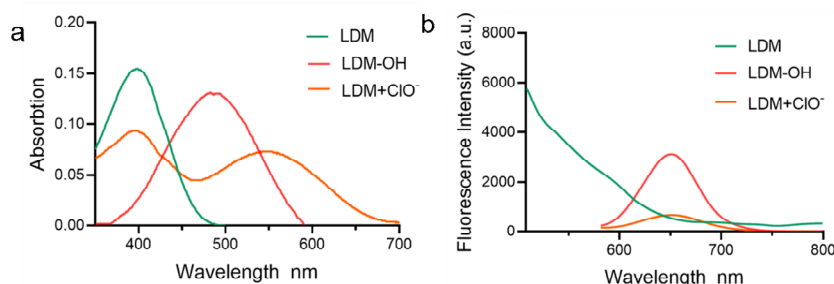
New Supplementary Figure18. The response of **LDM** to $\cdot\text{O}^{2-}$. **LDM** (10.0 μM) in different NaClO (100.0 μM) solution (DMSO-PBS,1:99, v/v, pH = 7.4). $\lambda_{\text{ex}} = 561\text{nm}$, slit: 10 nm/10 nm/700 V.

Comment 6: The author should give the UV-vis absorption spectra of **LDM**, **LDM-OH** and the reaction of **LDM** with ClO^- .

Response: Thank you for the reviewer's comments. We have supplemented the UV

absorption experiments of **LDM**, **LDM-OH** and the reaction of **LDM** with ClO^- . We add this result as new Supplementary Figure 15. **It reads now:**

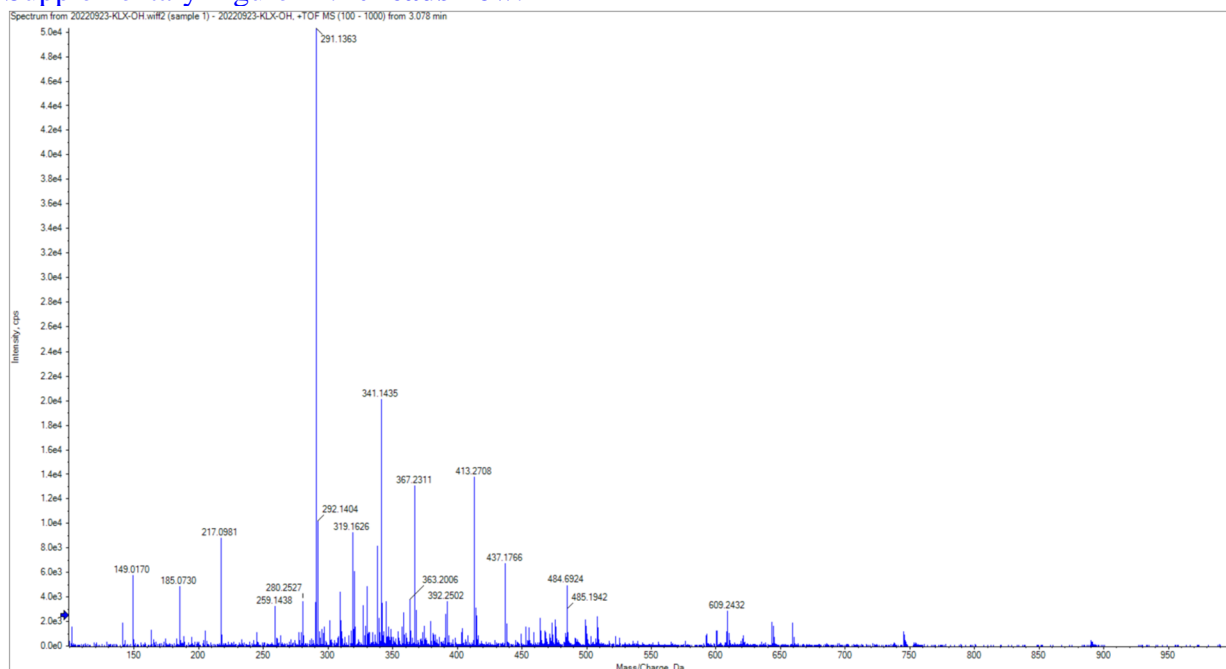
Line 114: **LDM** has a fast ability to respond to ClO^- (response time < 40 min). Additionally, we observed a decrease in absorption peak at 405 nm, and the new absorption peak that appears largely overlaps with the **LDM-OH** absorption peak, suggesting that **LDM** responds to HClO/ClO^- to generate **LDM-OH** *in vitro* (Supplementary Fig. 15).



New Supplementary Figure 15. (a) The UV absorption experiments of **LDM**, **LDM-OH** and the reaction of **LDM** with ClO^- . (b) The fluorescence intensity of **LDM**, **LDM-OH** and the reaction of **LDM** with ClO^- . **LDM:** $\lambda_{\text{ex}} = 488 \text{ nm}$, slit: 10 nm/10 nm/700 V. **LDM-OH:** $\lambda_{\text{ex}} = 561 \text{ nm}$, slit: 10 nm/10 nm/700 V.

Comment 7: It is recommended that the author change to a clearer version of Supplementary Figure 11.

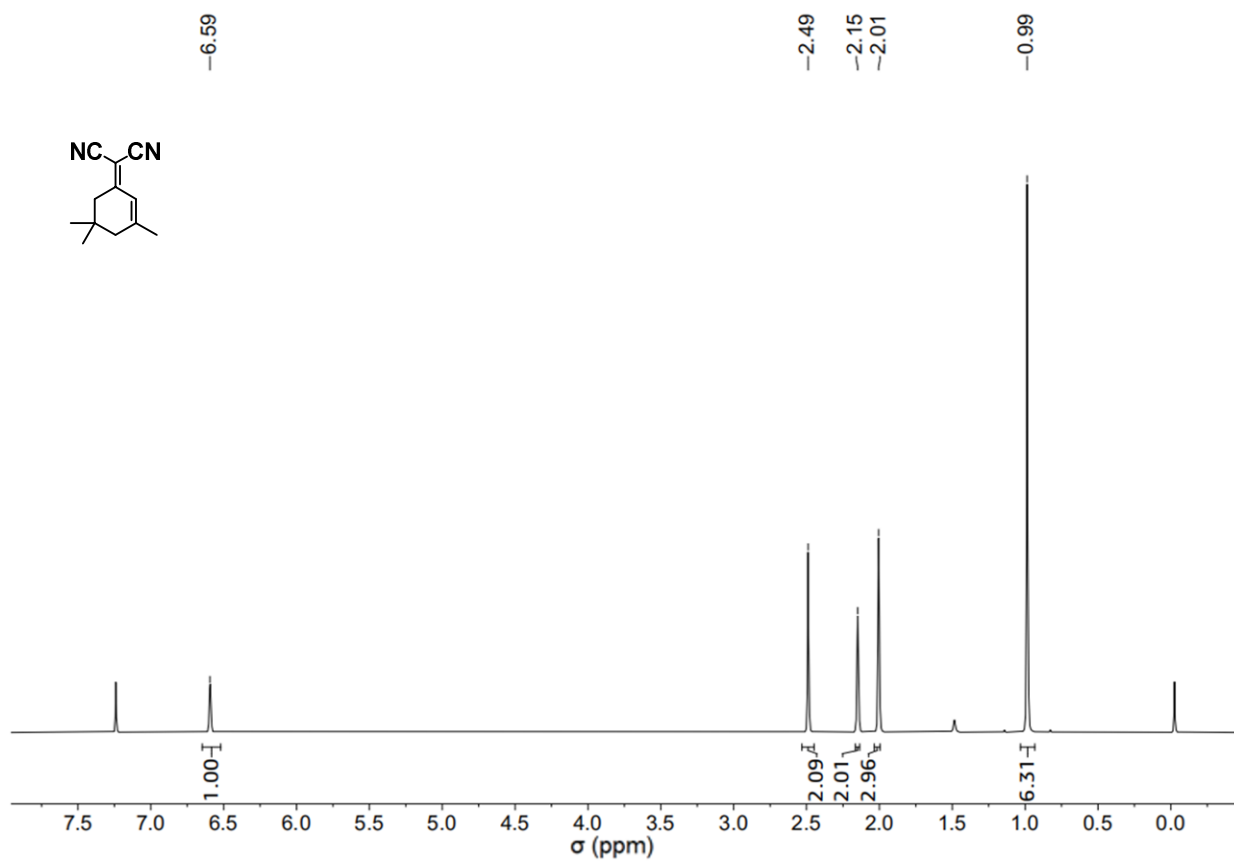
Response: Thank you for the review comments. We have replaced the clearer version of Supplementary Figure 11. **It reads now:**



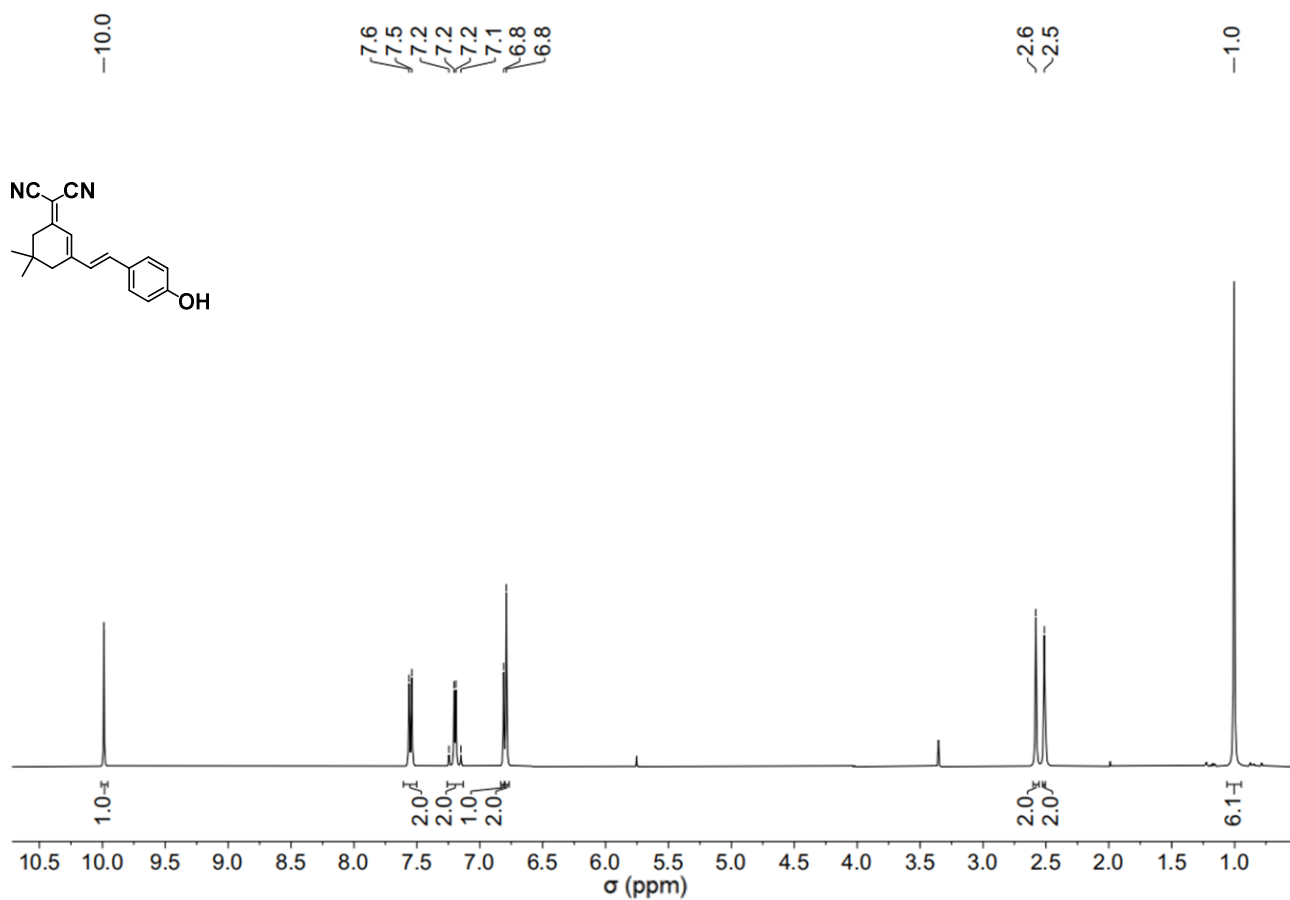
New Supplementary Figure 11. The HR-MS diagram of **LDM** ($10.0 \mu\text{M}$) and ClO^- ($100.0 \mu\text{M}$) reaction in DMSO-PBS buffer.

Comment 8: NMR characterization should be standardized, for example, the chemical shift unit (ppm) is missing.

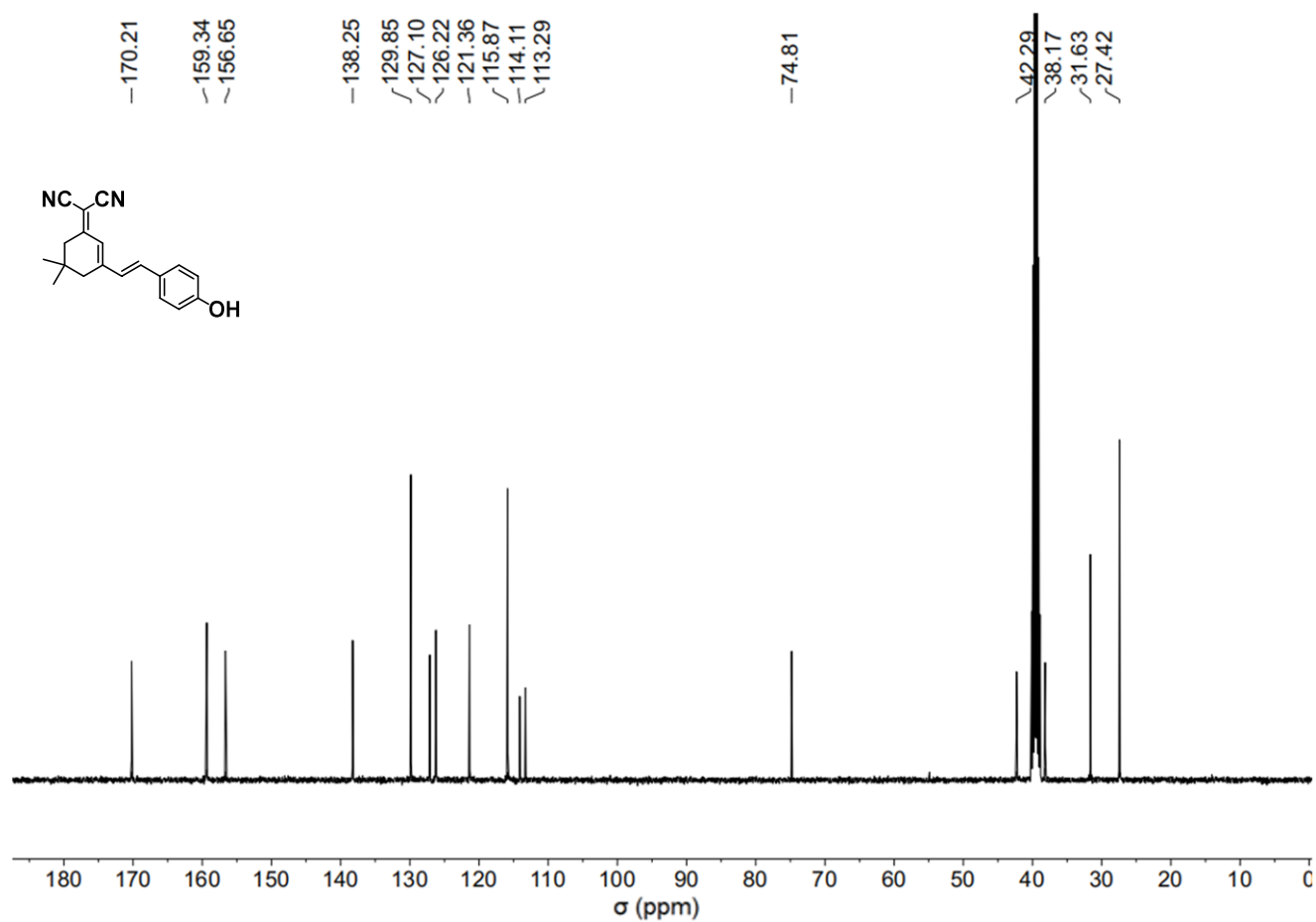
Response: Thank you for the reviewer's suggestions. We have made modifications and replacements to the nuclear magnetic spectrum. **It reads now:**



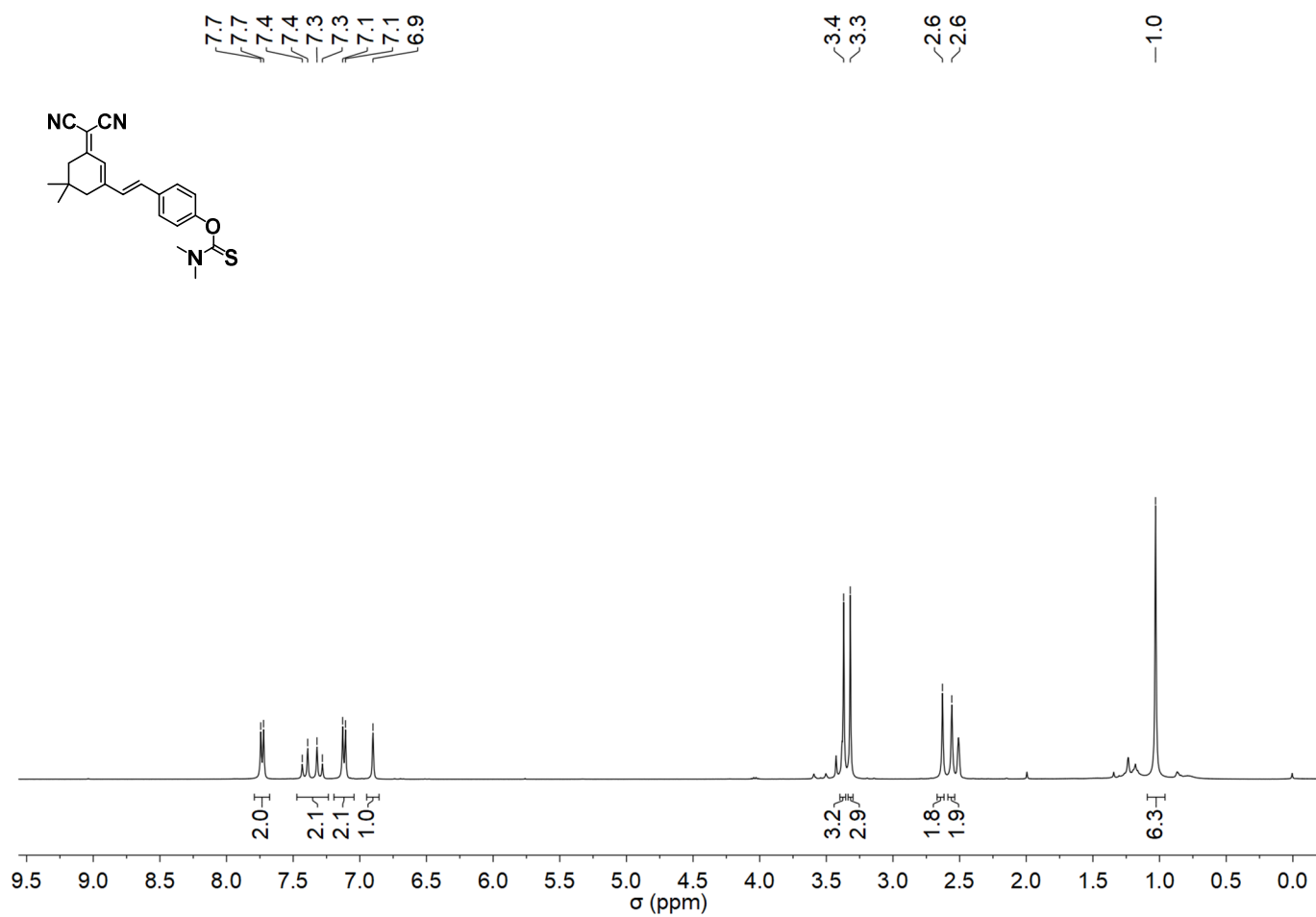
New Supplementary Figure 3. ¹H NMR spectra of compound 1.



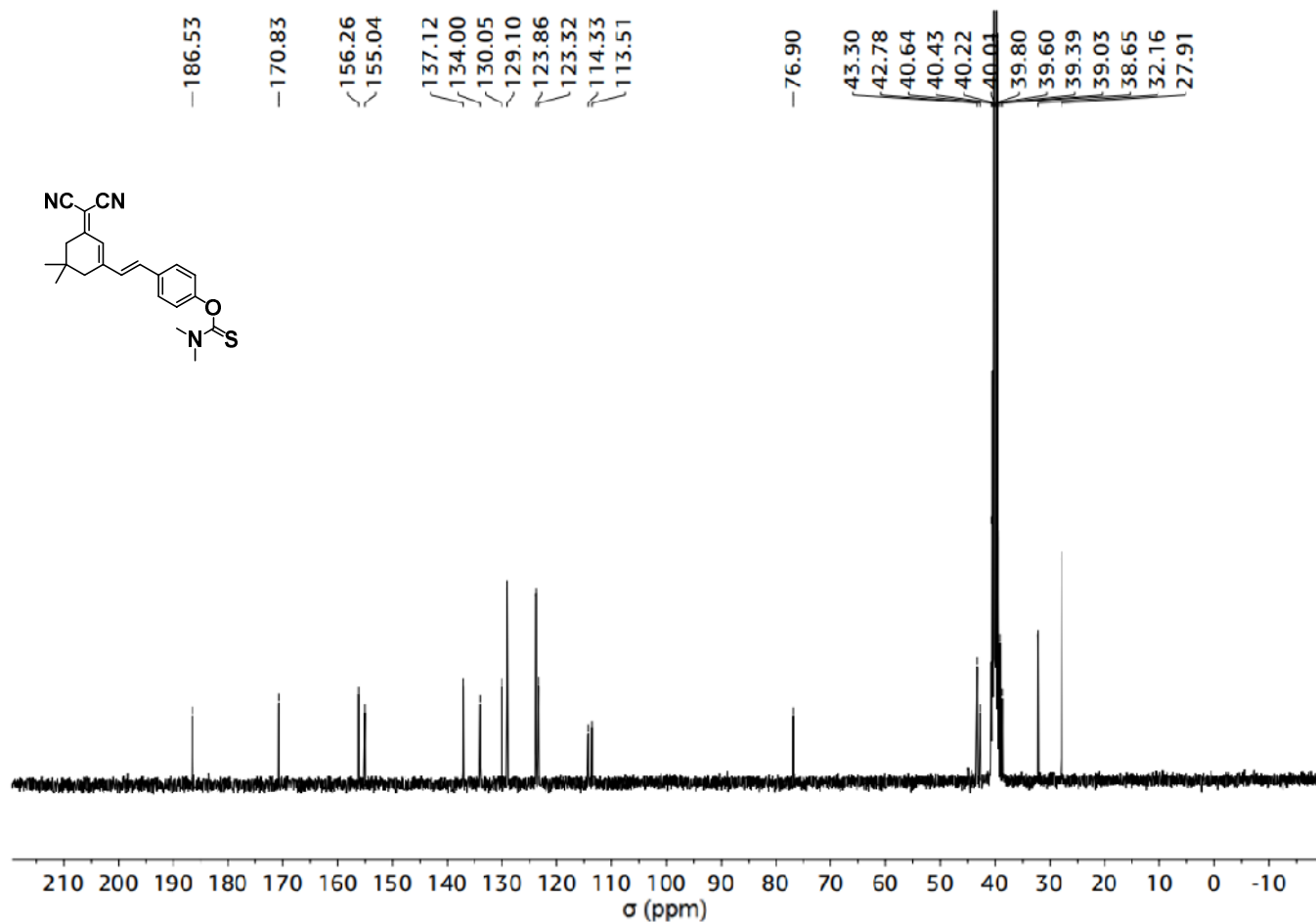
New Supplementary Figure 5. ^1H NMR spectra of compound **LDM-OH**.



New Supplementary Figure 6. ^{13}C -NMR spectra of compound **LDM-OH**.



New Supplementary Figure 8. ¹H NMR spectra of compound **LDM**.



New Supplementary Figure 9. $^{13}\text{C-NMR}$ spectra of compound **LDM**.

Comment 9: There are some errors in manuscript and ESI, including but not limited to: 1) Line 329, the author mentioned “DMSO-PBS, pH = 7.4, 1:1, v/v”, while in line 403 and 410, “DMSO-PBS, pH = 7.4, 1:99, v/v”.

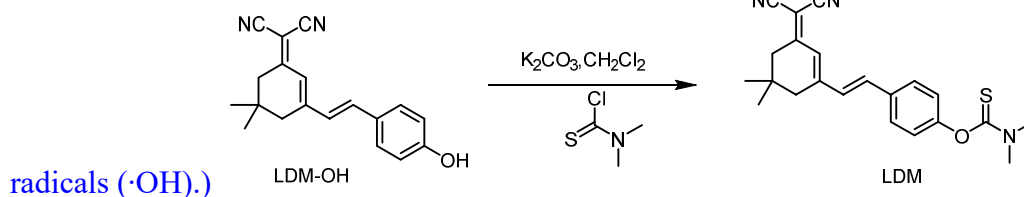
Response: Thank you for your suggestion. We have made some revisions in the manuscript and ESI. **It reads now:**

Line 369: Then dilute the stock solution to 10.0 μM with PBS (DMSO-PBS, pH = 7.4, 1:99, v/v), and record UV and fluorescence spectra at 37°C.

Comment 10: Supplementary Figure 10 does not correspond to line 324 of the manuscript. 3) Line 342, the author should confirm whether $(\text{NH}_4)_2\text{SO}_4 \cdot 6\text{H}_2\text{O}$ is $(\text{NH}_4)_2\text{Fe}(\text{SO}_4)_2 \cdot 6\text{H}_2\text{O}$?

Response: Thank you for your suggestion. We have changed to $(\text{NH}_4)_2\text{Fe}(\text{SO}_4)_2 \cdot 6\text{H}_2\text{O}$, and checked for other errors. **It reads now:**

Line 384: $(\text{NH}_4)_2\text{Fe}(\text{SO}_4)_2 \cdot 6\text{H}_2\text{O}$ mixed with 10 equivalents of H_2O_2 to prepare hydroxyl



New Supplementary Figure 2. Synthesis of **LDM**.

Reviewer #3 (Remarks to the Author):

This work from Kong et al. entitled “Molecular Probes for Tracking Lipid Droplet Membrane Dynamics 1” aims at developing a probe to label protein coats on LD specifically, by developing a new probe they called LDM. The synthesis and characterization of LDM, as shown in the first two figures, are well-executed.

We thank the reviewer for pointing out the “very positive attributes” of our manuscript. Meanwhile, her/his concerns have been addressed by additional experiments.

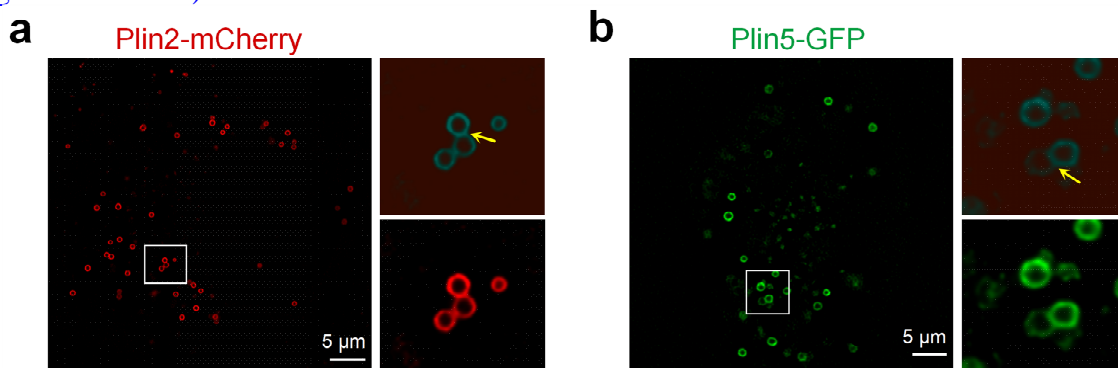
Comment 1: *However, the subsequent cellular usage, analysis and interpretation of LDM's recruitment to the LD surface, and its role in LD interactions or adhesion with mitochondria during energy demands, raise several concerns. Firstly, the differentiation between this approach and simply tagging proteins is unclear, except for the fact that the labeling in the author's method is non-specific. The physical and biological interpretations provided are premature and need substantial refinement. There are many other issues. I list some examples in the following.*

Response: We thank the reviewer for this frank and critical assessment. To address reviewer's concerns, a large amount of experiments were performed, including the comparison of the dynamics of non-specifically labeled LDs proteins (LDM) with specifically labeled LD proteins (Plin2-mCherry, Plin5-GFP, Cidec-GFP) when the LD membrane is close (new Fig. S27-28), assessing the accuracy of labeling LD membrane proteins by LDM under different resolutions of microscopes (new Fig. S29), and analyzing the dynamics of membrane proteins labeled by LDM when LD membranes are in contact or not (new Fig. S36). To further expand the application of LDM, we used LDM to evaluate the impact of drugs on LD-LD interaction, and to check drug's location under LD membranes (new Fig. S45-S46). These results further support that LDM is an attractive probe for labelling LD membranes under SIM in live cells.

Comment 2: *The statement "The uneven distribution might, therefore, be due to different protein distribution patterns within different red-like ring structures, particularly at the contact site," could be explained by the simple proximity of two droplets, which increases the signal in the contact.*

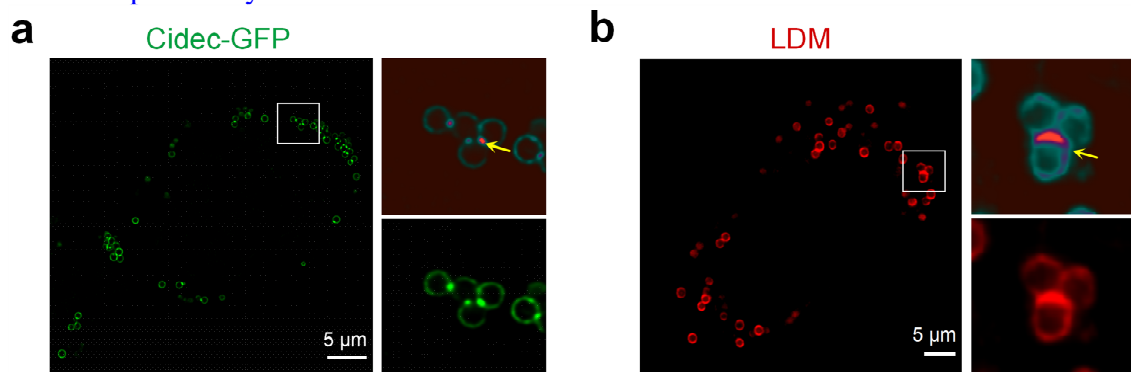
Response: We fully agree with the reviewer's comments. To confirm this, we further tested the reasons for this uneven distribution using several LD membrane proteins as control.

According to the literature, Plin2 and Plin5 proteins (*Biochimica et Biophysica Acta (BBA) - Molecular and Cell Biology of Lipids*, 2009, **1791**, 419-440; *Cell Death & Differentiation*, 2022, **29**, 2316-2331; *Journal of Biological Chemistry* 2024, **300**, doi:10.1016/j.jbc.2023.105610), known as uniform markers for LD membranes, were used as fluorescent markers for LDs. Our analysis revealed no significant fluorescence enrichment of Plin2 or Plin5 when LD membranes approached each other (as shown in New Supplementary Figure 27 a and b).



New Supplementary Figure 27. Fluorescent labeling of LD membranes with uniformly distributed proteins. **a.** SIM images of LD membrane proteins Plin2 (mCherry-labeled) when LD membranes approached each other, with the yellow arrows indicating the approaching regions. Representative images. **b.** SIM images of LD membrane proteins Plin5 (GFP-labeled) when LD membranes approached each other, with the yellow arrows indicating the approaching regions. Representative images. Plin5 -GFP channel: $\lambda_{ex} = 488$ nm; Plin2 mCherry channel: $\lambda_{ex} = 561$ nm.

To explore the possibility of specific protein aggregation, we test Cidec, a protein involved in LD fusion (*Dev Cell* 2021, **56**, 2592-2606), which distributes uniformly on single LD membranes but enriches membrane contact sites upon LD interactions. Remarkably, our **LDM** probe and labeled LD membranes accurately reflected this Cidec aggregation, with significant enrichment at membrane contact sites upon LD membrane proximity (as shown in new Supplementary Figure 28. a and b). This validates that the fluorescence enhancement observed with **LDM**-labeled LD membranes is not mere fluorescence overlap but an indicator of protein dynamics at membrane contact sites.



New Supplementary Figure 28. Fluorescent labeling of LD Membranes by mobile distribution proteins and LDM. **(a)** SIM images of LD membrane proteins Cidec (GFP-labeled) when LD membranes approached each other, with the yellow arrows indicating the approaching regions. **(b)** SIM images of **LDM** non-specifically labeled LD membrane proteins, when LD membranes approached each other, with the yellow arrows indicating the approaching regions. Cidec -GFP channel: $\lambda_{ex} = 488$ nm; **LDM** channel: $\lambda_{ex} = 561$ nm.

We have added these results to support our statement as the new Figure S27-28. **It reads now:**

Line 162: The uneven distribution might, therefore, be due to different protein distribution patterns within different red-like ring structures, particularly at the contact site. To further support that the **Plin2 and Plin5** proteins³⁴⁻³⁶, known as uniform markers for LD membranes, were used as fluorescent markers for LDs under SIM. Our analysis revealed no significant fluorescence enrichment of Plin2 or Plin5 when LD membranes approached each other (Supplementary Figure 27 a and b). To explore the possibility of specific protein aggregation, we next test Cidec³⁷, a protein involved in lipid fusion, which distributes uniformly on single LD membranes but enriches at membrane contact sites upon LD interactions. Remarkably, our **LDM** probe and labeled LD membranes accurately reflected this Cidec aggregation, with significant enrichment at membrane contact sites upon LD membrane proximity (Supplementary Figure 28 a and b). This validates that the fluorescence enhancement observed with **LDM**-labeled LD membranes is not mere fluorescence overlap but an indicator of protein dynamics at membrane contact sites.

Comment 3: "We also noticed that the fluorescence intensity of the **LDM**⁵⁶¹ marker at the contact site is more than twice that of the non-contact site (Supplementary Fig. 27)", suggesting that the high fluorescence intensity might be due to accumulation of labeled proteins at specific sites. The increased intensity could merely be due to the close proximity of two fluorescent interfaces, which would double the signal irrespective of adhesion.

Response: We fully agree with the reviewer's comment. According to the reviewer's suggestion, we provide an experiment (Supplementary Figure 28) as described in Reviewer #3 comment 2. The experiment verified that the fluorescence enhancement observed with LDM-labeled LD membranes is not mere fluorescence overlap but an indicator of protein dynamics at membrane contact sites. To address the reviewer's concern, we replaced the "adhesion" with a more accurate "accumulation" in the revised manuscript. **It reads now:**

Abstract section-Line 36: By utilizing **LDM**, we identified the dynamic mechanism of LD membrane contacts and their protein **accumulation** parameters. Furthermore, using **LDM** in liver cancer cells allowed us to examine the changes in LD/mitochondrial protein **accumulation**...

Introduction section-Line 78: By employing **LDM**, we shed light on the LD contact membrane protein **accumulation** in live cells, confirming dynamic mechanism of LD membrane contacts with mitochondria and their protein **accumulation** parameters. Furthermore, we investigated the protein **accumulation** parameters at the membrane contact....

Result section-Line190: **LDM** fluorescence aggregation as an indicator of membrane contact protein **accumulation** parameters.

Line 202: This result further validates **LDM**'s utility as a marker for protein **accumulation** between membrane contacts, reveals that protein **accumulation** may depend on increased co-localization of LD membrane proteins, and provides a tool for evaluating adhesion parameters in diverse cellular processes....

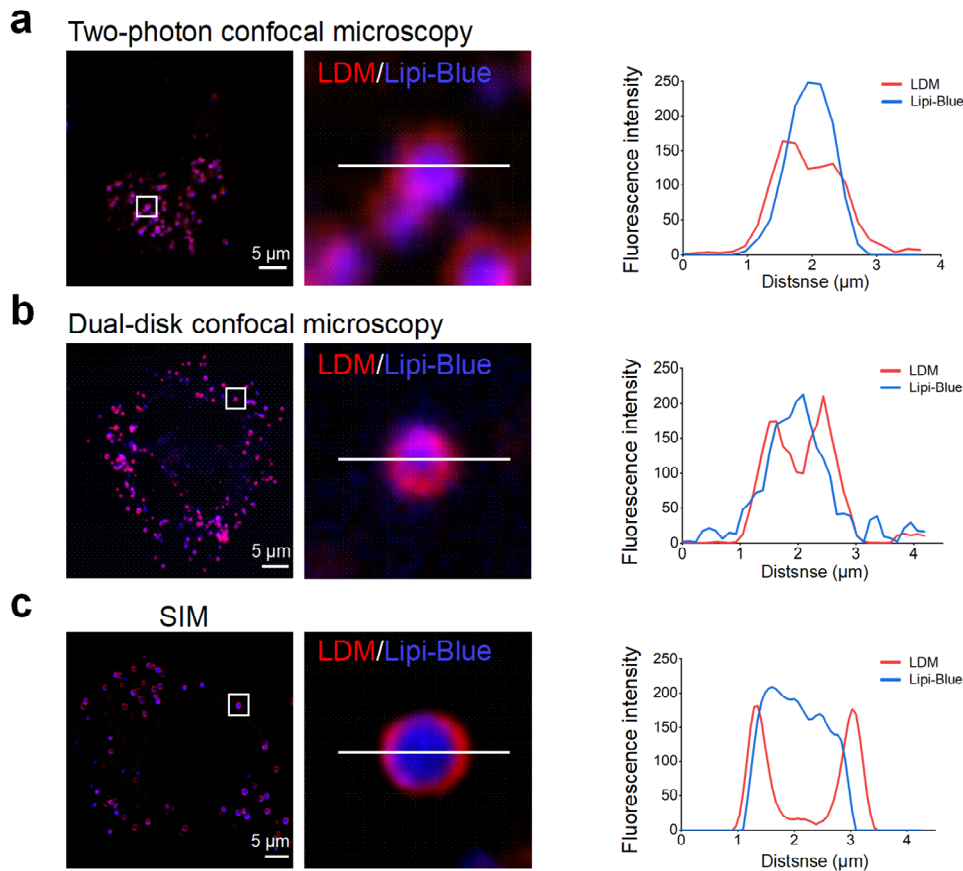
Line 214: To further verify the applicability of our probe to characterize the protein **accumulation** parameters, we further investigated the relationship between membrane protein **accumulation** and LD size.

Comment 4: "This suggests that the red ring-like structures labeled by **LDM** may represent the LD membrane." The lipid membrane of phospholipids is not the same as the protein coat. LDs are coated with peripheral proteins whose thickness in the cytosol varies. "Therefore, we believe that the size of the **LDM**-based ring is a more accurate representation of the LD size." This is not necessarily true, especially in cases where there is a thick protein coat.

Response: Response: We fully agree with the reviewer's comment that protein labeling on LDs membranes does not equate to phospholipid labeling. However, limitations in current cell fluorescence imaging techniques and lacking phospholipid labeling probe/plasmid, which prevent precise measurements of the true single-layer phospholipid membrane for LDs. Given that LDs proteins are integral to the droplet's envelope, we adopted an indirect approach by marking LDs membrane proteins to approximate LDs size. As a workaround, it may be more accurate compared to current probes targeting LD contents. Our analysis comparing two-photon confocal microscopy, dual-disk confocal microscopy, and SIM imaging techniques suggests that super-resolution microscopy-SIM offers a superior approximation of LD size (Supplementary Figure 29). We have revised the manuscript accordingly to address the reviewer's concerns. **It reads now:**

Line 173: This suggests that the red ring-like structures labeled by **LDM** using **SIM** may **close to** represent the LD membrane (Supplementary Figure 29).

Line 182: Therefore, we believe that the size of the **LDM-based ring under SIM** is a more accurate representation of the LD size, **compare to traditional microscopy**.

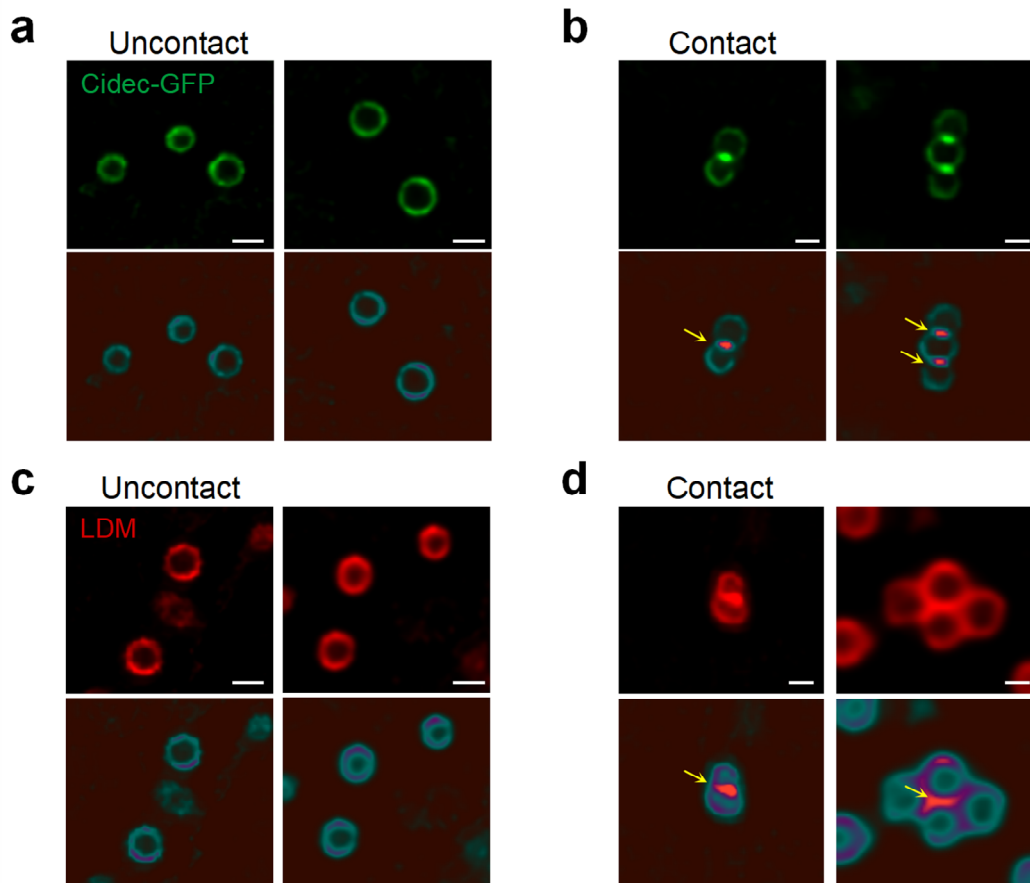


New Supplementary Figure 29. Membrane of LDs labeled by LDM under different resolutions of microscopes (a) Two-photon confocal microscopy images of LDs labeled with Lipi-Blue and the LD membrane protein layer labeled with **LDM**, as well as the fluorescence curve at the white line. Representative images. **(b)** Dual-disk confocal microscope images of LDs labeled with Lipi-Blue and LD membrane protein layer labeled with **LDM**, as well as the fluorescence curve at the white line. Representative images. **(c)** Super-resolution microscopy (SIM) images of LDs labeled with Lipi-Blue and LD membrane protein layer labeled with **LDM**, as well as the fluorescence curve at the white line. Representative images. Lipi-Blue channel: $\lambda_{\text{ex}} = 405 \text{ nm}$; LDM channel: $\lambda_{\text{ex}} = 561 \text{ nm}$.

Comment 5: "Consequently, we propose that our probe captures the real contact sites between multiple LD interactions in living cells (Fig. 3g)." This conclusion lacks sufficient convincing evidence and, again, proximity does not necessarily reflect contact sites.

Response: We fully concur with the reviewer's perspective that proximity does not equate to authenticity. During LD contact, it is the outer membrane proteins that initially undergo changes. To validate that our probe captures the precise contact sites, we examined Cidec protein, a key player in LD contact and fusion (*Dev Cell* 2021, **56**, 2592-2606). Under physiological conditions, Cidec protein is uniformly distributed on LD membranes, as shown in Supplementary Figure 36 a, with a relatively even distribution of fluorescence intensity. However, upon LD contact, Cidec protein accumulates at the contact sites (Supplementary Figure 36 b). Our **LDM** probe exhibits a similar pattern, with significant enrichment at membrane contact sites during LDM-membrane interaction, as depicted in Supplementary Figure 36 c-d. To address the reviewer's concern, we also add this result as new Supplementary Figure 36, and have revised our statement accordingly. **It reads now:**

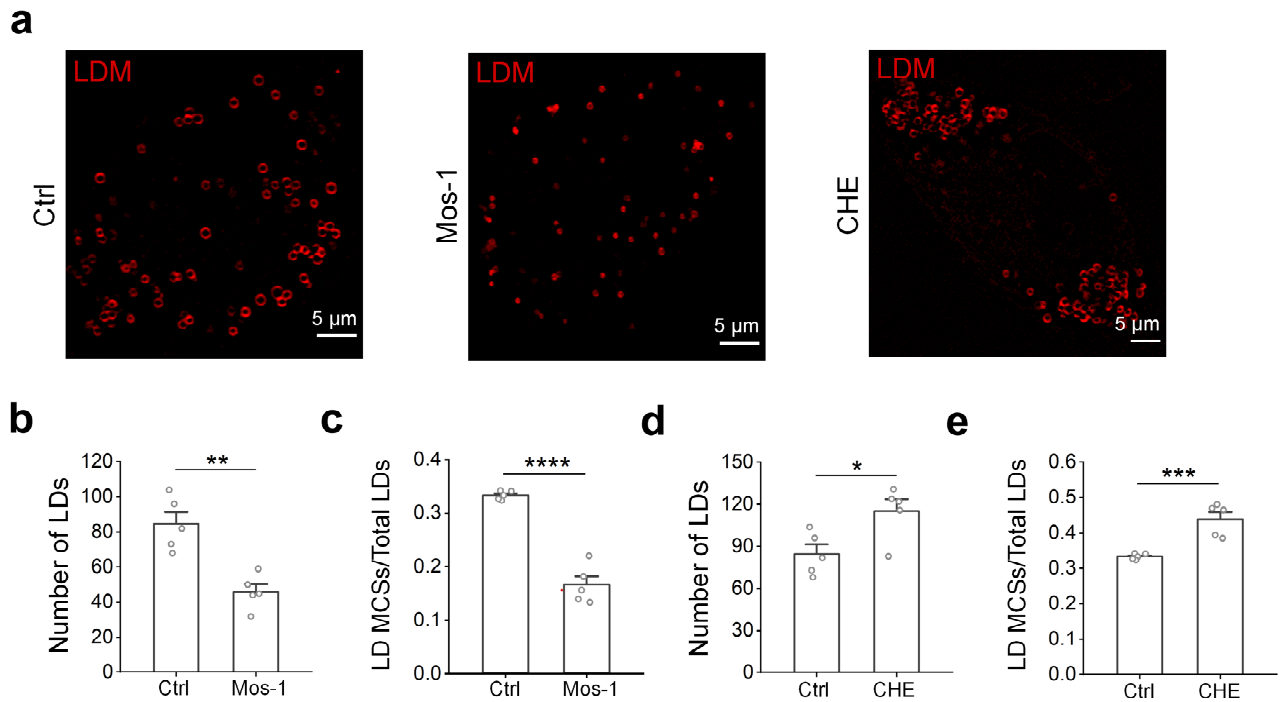
Line 186: Consequently, we propose that our probe captures the **more precise** contact sites between multiple LD interactions in living cells (Fig. 3g, **Supplementary Figure 36**), compared to probe labeling technology located in the LD core (**Supplementary Figure 29** and **Supplementary Figure 32**).



New Supplementary Figure 36. The dynamics of Cidec-GFP and LDM labeled LD membrane proteins during non-contact and contact periods. (a) SIM image of the distribution of LD membrane protein Cidec-GFP on the surface of LDs (without membrane contact). Representative images. Scale bars, 1 μm . (b) Super-resolution microscopy image of the distribution of LD membrane protein Cidec-GFP on the surface of LDs (membrane contact), with the yellow arrows indicating the approaching regions. Representative images. Scale bars, 1 μm . (c) Super-resolution microscopy image of the distribution of LD membrane protein layer with **LDM** non-specific labeling on the LD (without membrane contact) membrane. Representative images. Scale bars, 1 μm . (d) Super-resolution microscopy image of the distribution of LD membrane protein layer with **LDM** non-specific labeling on the LD (membrane contact) membrane, with the yellow arrows indicating the approaching regions. Representative images. Scale bars, 1 μm . Cidec -GFP channel: $\lambda_{\text{ex}} = 488 \text{ nm}$; LDM channel: $\lambda_{\text{ex}} = 561 \text{ nm}$.

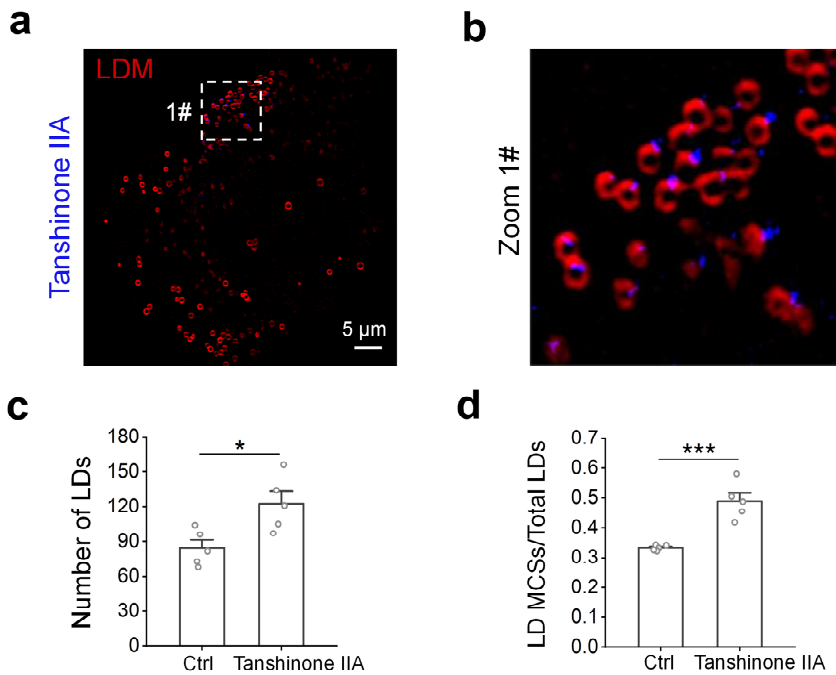
Comment 6: *This referee encourages the authors to revisit the interpretations and conclusions drawn from your data and to think more about the valorization of their tool.*

Response: We appreciate the reviewer's feedback and have made revisions to address these inaccurate statements. In addition to its role in cellular processes (Figure 5), we have explored our tool's potential in drug evaluation. Testing known LD modulators Mos-1, CHE, and tanshinone IIA revealed Mos-1 reduces LD numbers and contact, while CHE increases LD numbers but reduces contact (Supplementary Figure 45), consistent with prior reports⁴².



New Supplementary Figure 45. Utilizing LDM to assess drug effects on LD and LD interaction. (a) The changes of LDs marked by LDM in the Ctrl group, the mussel oligosaccharides (Mos-1) group (100 μ M, 24 h), and the chelerythrine (CHE) group (1 μ M, 24 h). SIM imaging. Representative images. (b) Comparison of LD numbers between Ctrl and Mos-1 groups. $n = 5$. (c) Comparison of the ratio of membrane contact sites (MCSs) to total number of LDs between Ctrl and Mos-1 groups. $n = 5$. (d) Comparison of LD numbers between Ctrl and CHE groups. $n = 5$. (e) Comparison of the ratio of MCSs to total number of LDs between Ctrl and CHE groups. $n = 5$. Data are shown as mean \pm SE ($*p < 0.05$, $**p < 0.01$, $***p < 0.001$, $****p < 0.0001$). LDM channel: $\lambda_{ex} = 561$ nm.

Notably, our examination of tanshinone IIA with autofluorescence showed it enhances LD numbers, contact, and exhibits a LD membrane localization labeled by our probe (Supplementary Figure 46). These findings provide an attractive tool for further investigations into the specific regulatory LD related metabolism diseases drug. We add this result as new Supplementary Figure 45 and Supplementary Figure 46.



New Supplementary Figure 46. Using LDM to evaluate the effect of drugs on LD interaction and check the drug's location in the LD membrane. (a-b) After treatment with 1 μ M Tanshinone IIA (Blue) for 24 h, changes in LDs labeled by LDM. SIM imaging. Representative images. (c) Comparison of LD numbers between Ctrl and tanshinone IIA groups. $n = 5$. (d) Comparison of the ratio of MCSs to total number of LDs between Ctrl and tanshinone IIA groups. $n = 5$. Data are shown as mean \pm SE (* $p < 0.05$, ** $p < 0.01$, *** $p < 0.001$, **** $p < 0.0001$). Tanshinone IIA channel: $\lambda_{ex} = 405$ nm; LDM channel: $\lambda_{ex} = 561$ nm.

It reads now:

Line 257: Subsequently, these LDs release FAs, migrate to mitochondria, and are oxidized by mitochondria, thereby providing energy for starving cancer cells (Fig. 5n). **In addition to its role in cellular processes, we have explored our tool's potential in drug evaluation. Testing known LD modulators Mos-1⁴⁹, CHE⁵⁰, and tanshinone IIA⁵¹ revealed Mos-1 reduces LD numbers and contact, while CHE increases LD numbers but reduces contact (Supplementary Figure 45), consistent with prior reports. Notably, our examination of tanshinone IIA with autofluorescence showed it enhances LD numbers, contact, and exhibits a membrane localization labeled by our probe (Supplementary Figure 46). In summary, we used LDM to label LD membranes of liver cancer cells during the period of starvation, drug evaluation, and the drug location. These applications provide an attractive tool for further investigations into the specific regulatory mechanisms and drug discovery associated with LD related metabolism diseases.**

REVIEWER COMMENTS

Reviewer #1 (Remarks to the Author):

I am satisfied with the author's revisions to the paper and recommend that it be accepted and published.

Reviewer #2 (Remarks to the Author):

As I mentioned in my previous review, this work is novel and the present revised manuscript still has some doubts that need further explanation by the authors, so it is suitable for publication in Nature Communications after the following comments are addressed.

1, The author used Rhodamine B as the standard for fluorescence quantum yield, and Φ_{R-B} in ethanol is 0.82. Please provide the corresponding reference. In addition, in the calculation formula of relative quantum yield, FLDM and FR-B are the integrated fluorescence intensities of LDM and Rhodamine B, respectively. The absorbance value required by the formula should generally be less than 0.05. The authors should check the excitation wavelengths of LDM and Rhodamine B, and provide the fluorescence quantum yield of LDM with or without ClO⁻ in the system (DMSO-PBS, 1:99, v/v, pH=7.4). In New Supplementary Figure 14, the fluorescence spectrum of LDM is incorrect, and the authors should confirm whether Rhodamine B used as a standard is in methanol or ethanol?

2, As shown in Supplementary Figure 16, both LDM and LDM-OH show an increase in fluorescence intensity with increasing viscosity or decreasing polarity. Will this have a certain impact on subsequent cell imaging?

3, Compared with the existing fluorescent probes for detecting ClO⁻ (Sensor Actuat. B-Chem. 2021, 343, 130063; Anal. Chem. 2024, 96, 5428–5436), the response time of LDM to ClO⁻ is relatively long, so it is inappropriate for the author to mention "LDM has a fast ability to respond to ClO⁻" in the article.

4, In Supplementary Figure 18, the green line of 0 μ M was not observed, and the fluorescence intensity in Supplementary Figure 18 was significantly higher than that in Supplementary Figure 17. It is suggested that the testing conditions of superoxide ion are consistent with those of various other ions in Supplementary Figure 17.

5, Theoretically, LDM reacts with ClO⁻ to generate LDM-OH. However, as shown in Supplementary Figure 15, the absorption wavelength of LDM after reacting with ClO⁻ is not consistent with that of LDM-OH. In addition, the maximum absorption wavelength of LDM is about 400 nm, but its excitation wavelength is 488 nm. Similarly, the maximum absorption wavelength of LDM-OH is about 488nm, but its excitation wavelength is 561 nm. The author should provide corresponding explanations.

Reviewer #3 (Remarks to the Author):

The authors have made significant efforts to address the referee's comments, resulting in a good improvement to the manuscript. Most of my initial concerns have been qualitatively addressed. However, there are still some points that either remain unclear regarding the mechanism by which LDM functions at contact sites or that this referee may not fully understand. Despite my limited expertise in organic chemistry (which, while not essential for evaluating this work, may be contributing to this confusion), I believe that an important aspect of how LDM operates when two objects are in close proximity is missing from the manuscript.

This issue could be clarified through two approaches, both of which do not require additional experiments:

1. Systematic LDM Signal Increase at LD-LD Contacts: Does LDM labeling consistently result in an increased signal at LD contact sites? Specifically, what fraction of LD-LD contacts exhibit enhanced LDM signals? If this phenomenon occurs systematically, it raises the possibility that LDM may be promoting these contacts.
2. Comparison with CIDEDEC-Induced Contacts: The authors have compared LDM's behavior to that of CIDEDEC, which is known to induce contact sites. Therefore, it is crucial to consider whether LDM might also induce artificial contact sites. To address this, the authors should quantify the number of LD clusters formed when using PLIN2, PLIN5, or CIDEDEC compared to LDM. If more clustering is observed with LDM, it strongly suggests that LDM could be inducing artificial contacts. This could occur if LDM on one LD surface attaches to proteins on a neighboring LD or organelle surface. In this case, LDM might be actively inducing

contact sites beyond labeling the LD surface.

These points only require simple quantifications, not additional experiments, which the authors have already conducted extensively. My intention is not to be overly critical or subjective but to ensure that the authors present tools that can genuinely advance research in this field. The work done so far is indeed impressive, and I believe addressing these points will further strengthen the manuscript.

Response to the review comments

We thank the Reviewer #1 for accepting our manuscript for publication. We also thank the Reviewer #2 and #3 for their constructive criticism. We have revised the manuscript accordingly and all of their concerns were addressed by appropriate revision of the text. We believe the manuscript greatly improved in its rigor and presentation thanks to the reviewers' help.

Reviewer #1 (Remarks to the Author):

I am satisfied with the author's revisions to the paper and recommend that it be accepted and published.

We thank the reviewer for the positive and encouraging notes on our efforts to improve the manuscript.

Reviewer #2 (Remarks to the Author):

As I mentioned in my previous review, this work is novel and the present revised manuscript still has some doubts that need further explanation by the authors, so it is suitable for publication in Nature Communications after the following comments are addressed.

We thank the reviewer for the positive note on our manuscript, and appreciate valuable comments.

Comment 1: *The author used Rhodamine B as the standard for fluorescence quantum yield, and Φ_{R-B} in ethanol is 0.82. Please provide the corresponding reference. In addition, in the calculation formula of relative quantum yield, F_{LDM} and F_{R-B} are the integrated fluorescence intensities of **LDM** and Rhodamine B, respectively. The absorbance value required by the formula should generally be less than 0.05. The authors should check the excitation wavelengths of **LDM** and Rhodamine B, and provide the fluorescence quantum yield of **LDM** with or without ClO^- in the system (DMSO-PBS, 1:99, v/v, pH=7.4). In New Supplementary Figure 14, the fluorescence spectrum of **LDM** is incorrect, and the authors should confirm whether Rhodamine B used as a standard is in methanol or ethanol?*

Response: According to reviewer comments, we supplemented the fluorescence quantum yield of **LDM** with and without ClO^- in the system (DMSO-PBS, 1:99, v/v, pH=7.4). The fluorescence quantum yield of **LDM** was calculated by the following equation:

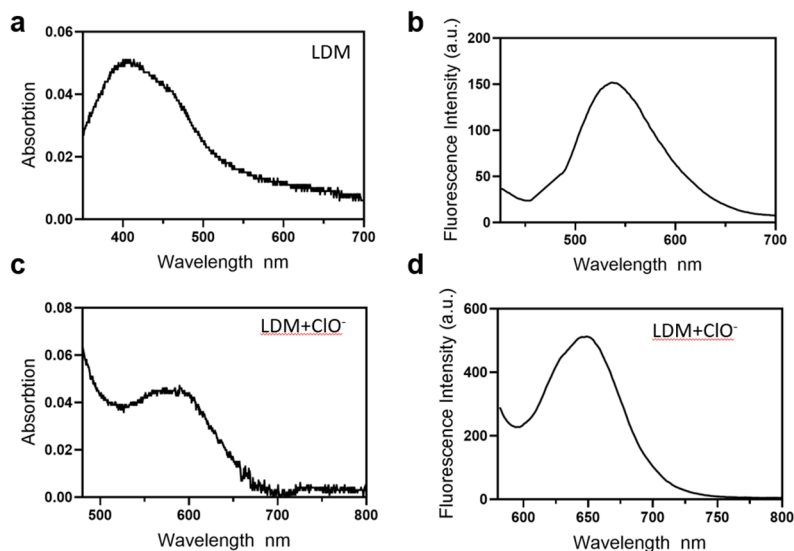
$$\Phi_{LDM} = \frac{\Phi_{R-G} \times F_{LDM} \times A_{R-G}}{F_{R-G} \times A_{LDM}}$$

where Φ_{LDM} represents the fluorescence quantum yield of **LDM** and Φ_{R-G} is the fluorescence quantum yield of the standard rhodamine 6G (rhodamine 6G in ethanol $\Phi = 0.95$); Integral area of fluorescence intensity at 405 nm and 530 nm excitation for F_{LDM} and F_{R-B} , respectively; A_{LDM} and A_{R-B} are absorbance at fixed excitation wavelengths ($A < 0.05$). The fluorescence quantum yield was 0.16. The addition of NaClO to the **LDM** solution resulted in a new absorption peak at 561 nm, and similarly, we calculated the fluorescence quantum yield of **LDM** with NaClO, and the fluorescence quantum yield was: 0.37.

We apologize for this confusion, and we have checked and revised the manuscript. Rhodamine 6G was chosen as the standard for this experiment, and the fluorescence quantum yield of rhodamine 6G was about

0.95. (*Photochem. Photobiol.* 2002, 75, 327; *Pure Appl. Chem.*, 2011, 83, 2213). We have checked and updated the Supplementary Fig. 14. **It reads now:**

Line 112: “The **LDM** to ClO^- reaction was completed in 40 min (Supplementary Fig. 13), with a fluorescence quantum yield of 0.37 (Supplementary Fig. 14).



Updated Supplementary Fig. 14. Absorption and fluorescence spectra during fluorescence quantum yield measurements. (a) UV absorption spectrum of **LDM** (DMSO-PBS, 1:99, v/v). (b) Fluorescence spectrum of **LDM** in deionized water, $\lambda_{\text{ex}} = 405$ nm. (c) UV absorption spectrum of **LDM** + ClO^- . (d) Fluorescence spectrum of **LDM** + ClO^- , $\lambda_{\text{ex}} = 561$ nm.

Comment 2: As shown in Supplementary Figure 16, both **LDM** and **LDM-OH** show an increase in fluorescence intensity with increasing viscosity or decreasing polarity. Will this have a certain impact on subsequent cell imaging?

Response: Thank you for your valuable comment. We fully agree that the reviewer's point is crucial for LD imaging. Indeed, many LD probes (*Chem. Sci.*, 2019, 10, 2342–2349; *Angew. Chem., Int. Ed.*, 2021, 60, 25104–25113) labeled with LD contents exhibit interference from the polarity and viscosity of the lipid droplet core. However, our probe is specifically positioned on the lipid droplet membrane. Based on our experimental results (Fig 3a and Fig 4e), no significant difference was observed in the imaging of the lipid droplet membrane between the normal and drug-induced treatment groups.

Comment 3: Compared with the existing fluorescent probes for detecting ClO^- (*Sensor Actuat. B-Chem.* 2021, 343, 130063; *Anal. Chem.* 2024, 96, 5428–5436), the response time of **LDM** to ClO^- is relatively long, so it is inappropriate for the author to mention “**LDM** has a fast ability to respond to ClO^- ” in the article.

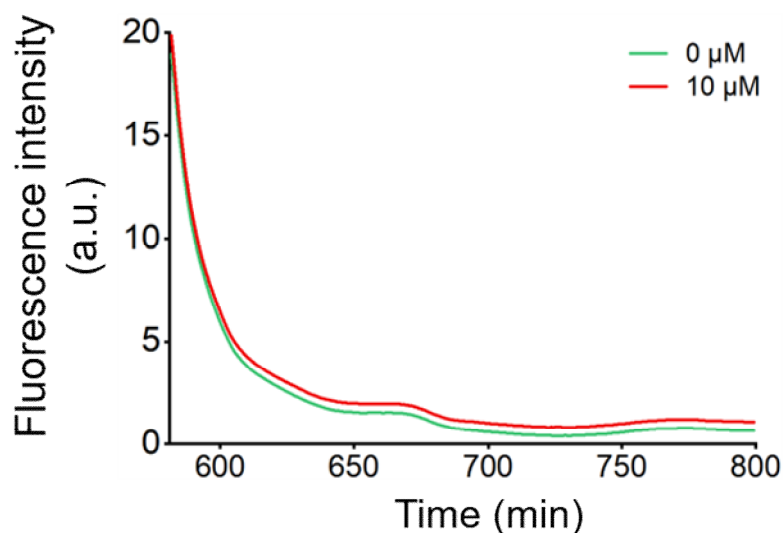
Response: According to reviewer comments, we have revised this statement. **It reads now:**

Line 112: “The **LDM** to ClO^- reaction was completed in 40 minutes.”

Comment 4: In Supplementary Figure 18, the green line of 0 μM was not observed, and the fluorescence intensity in Supplementary Figure 18 was significantly higher than that in Supplementary Figure 17. It is

suggested that the testing conditions of superoxide ion are consistent with those of various other ions in Supplementary Figure 17.

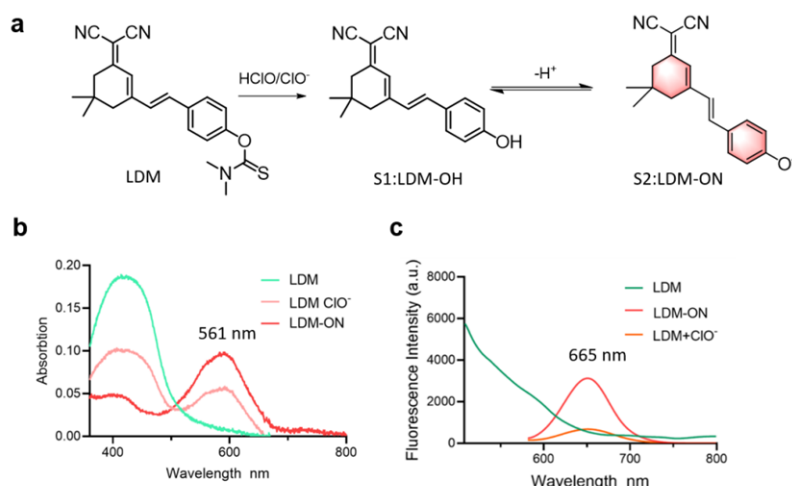
Response: Thank you for your suggestion. According to reviewer comments, we retested and provided new results under the same testing conditions as updated Supplementary Figure 18.



Updated Supplementary Figure 18. The response of **LDM** to $\cdot\text{O}_2^-$. **LDM** (10.0 μM) in different NaClO (100.0 μM) solution (DMSO-PBS, 1:99, v/v, pH = 7.4). $\lambda_{\text{exc}} = 561\text{ nm}$, slit: 5 nm/5 nm/700 V.

Comment 5: Theoretically, **LDM** reacts with ClO^- to generate **LDM-OH**. However, as shown in Supplementary Figure 15, the absorption wavelength of **LDM** after reacting with ClO^- is not consistent with that of **LDM-OH**.

Response: We apologize for this confusion. The inconsistency between the absorption wavelength of **LDM** after reacting with ClO^- and that of **LDM-OH** is likely due to the unaccounted effects of the microenvironment on compound dissociation. Literature suggests that under neutral or slightly alkaline conditions, **LDM-OH** can dissociate into **LDM-ON**. This process is enhanced by DMSO and is most effective in a PBS/DMSO buffer (pH 7.4, 1:1, v/v) (*Sensors & Actuators: B. Chemical* 293 (2019) 265-27). In our *in vitro* tests using a DMSO-PBS (1:99, v/v) solution, the reaction with NaClO under these slightly alkaline conditions promoted deprotonation, leading to a new absorption peak at 561 nm and NIR emission at 665 nm. These spectral properties are presented in Updated Supplementary Figure 15. Here, we have standardized the references to **LDM-OH** as state 1 and **LDM-ON** as state 2. In this manuscript, **LDM-OH** is harmonized into the written forms of state 1 and state 2.



Updated Supplementary Figure 15. (a) The structure of probe **LDM** and its fluorescence response mechanism towards NaClO. (b) The UV spectra changes of **LDM**, **LDM** with additional NaClO and **LDM-ON**. (c) The fluorescence spectra changes of **LDM** (10 μM) with additional NaClO (λ_{ex} : 488/561 nm).

Comment 6: In addition, the maximum absorption wavelength of **LDM** is about 400 nm, but its excitation wavelength is 488 nm. Similarly, the maximum absorption wavelength of **LDM-OH** is about 488 nm, but its excitation wavelength is 561 nm. The author should provide corresponding explanations.

Response: We conducted a cell imaging study to evaluate the fluorescence excitation wavelength of **LDM**. Our results indicate that **LDM** exhibits weaker fluorescence at 405 nm but significantly better fluorescence intensity at 488 nm. As shown in Figure 1, the 488 nm excitation provided clearer imaging, leading us to select 488 nm as the optimal excitation wavelength for **LDM**.

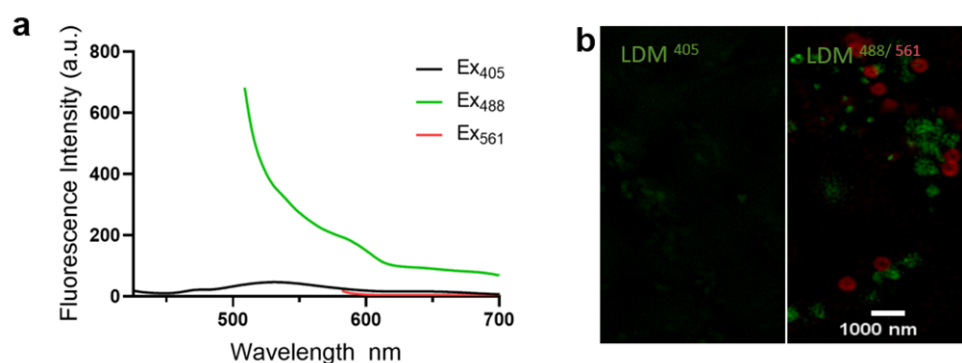


Figure 1. (a) Fluorescence spectra of **LDM** upon excitation at 405 nm, 488 nm, and 561 nm, respectively. (b) Cellular imaging of **LDM**-incubated HepG2 cells incubated with **LDM** for 1h upon excitation at 405 nm, 488 nm, 561 nm, respectively.

Reviewer #3 (Remarks to the Author):

The authors have made significant efforts to address the referee's comments, resulting in a good improvement to the manuscript. Most of my initial concerns have been qualitatively addressed. However, there are still some points that either remain unclear regarding the mechanism by which **LDM** functions at contact sites or that this referee may not fully understand. Despite my limited expertise in organic chemistry (which, while not essential for evaluating this work, may be contributing to this confusion), I believe that an important aspect of how **LDM** operates when two objects are in close proximity is missing from the manuscript.

This issue could be clarified through two approaches, both of which do not require additional experiments:

We thank the reviewer for the recognition on our manuscript and valuable comments.

Comment 1: Systematic **LDM** Signal Increase at LD-LD Contacts: Does **LDM** labeling consistently result in an increased signal at LD contact sites? Specifically, what fraction of LD-LD contacts exhibit enhanced **LDM** signals? If this phenomenon occurs systematically, it raises the possibility that **LDM** may be promoting these contacts.

Response: Thank you for your advice. According to reviewer comments, we conducted a quantitative analysis of **LDM** signal intensity at LD membrane contact sites under various nutritional conditions, including starvation, normal state, and incubation with added oleic acid. The imaging results are presented in Figure 2a. Our findings indicate that the enrichment of **LDM** between LDs is positively correlated with the nutritional status of the cells; that is, when cells are storing lipids (and the contact-fusion of LDs is enhanced), **LDM** is more likely to accumulate between the LDs. Additionally, we statistically analyzed the fluorescence intensity at the contact sites, with the statistical framework illustrated in Figure 2b. Our data suggest that **LDM** labeling does not consistently result in increased signal intensity at LD contact sites.

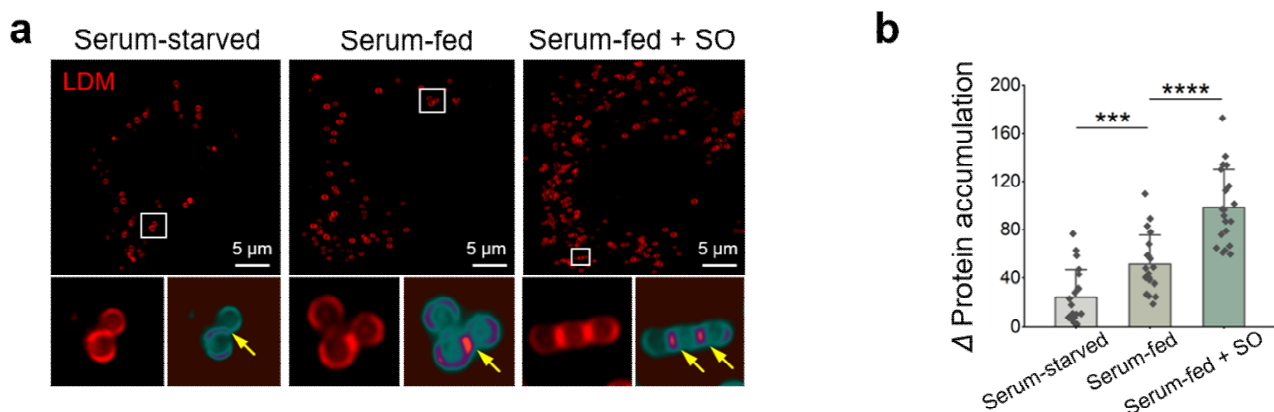


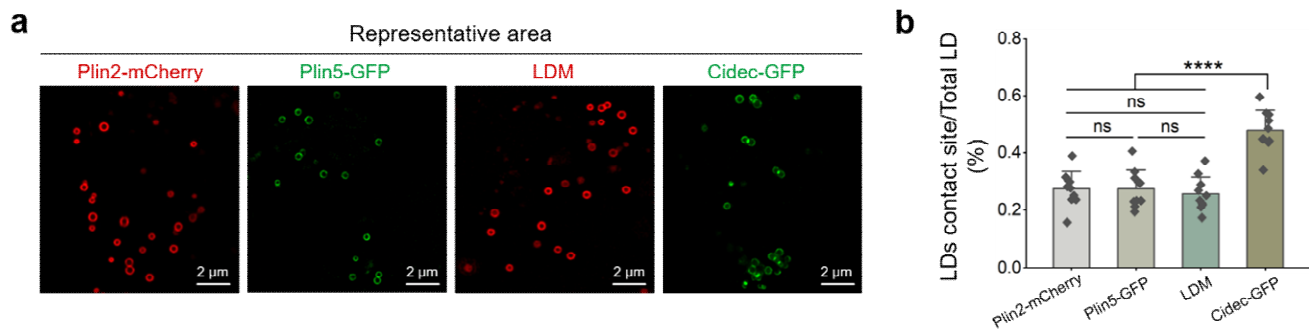
Figure 2: SIM images of HepG2 cells labeling LDs with **LDM** under serum-starved, serum-fed, and serum-fed + sodium oleic (SO) conditions. (a) Representative images. (b) Under different nutritional conditions, quantitative analysis of **LDM** enrichment in the contact sites of LDs in HepG2 cells. $n = 20$. Data are shown as mean \pm SD (***) $p < 0.001$, **** $p < 0.0001$).

Comment 2: Comparison with CIDEA-Induced Contacts: The authors have compared **LDM**'s behavior to

that of CIDEC, which is known to induce contact sites. Therefore, it is crucial to consider whether **LDM** might also induce artificial contact sites. To address this, the authors should quantify the number of LD clusters formed when using PLIN2, PLIN5, or CIDEC compared to **LDM**. If more clustering is observed with **LDM**, it strongly suggests that **LDM** could be inducing artificial contacts. This could occur if **LDM** on one LD surface attaches to proteins on a neighboring LD or organelle surface. In this case, **LDM** might be actively inducing contact sites beyond labeling the LD surface.

Response: Thank you for your suggestion. According to reviewer comments, we have quantified the number of LD clusters formed by PLIN2, PLIN5, and CIDEC compared to **LDM**, respectively. CIDEC, a known contact site-inducing substance, induced an increase in contact sites. However, PLIN2, PLIN5, and **LDM** labeling results revealed no significant difference in the number of lipid droplet contacts. Therefore, **LDM** does not actively induce contact sites on the surface of lipid droplets while labeling LD. We added this result as New Supplementary Fig. 37. **It reads now:**

Line 189: Furthermore, the **LDM** alone does not trigger the formation of LD membrane contact sites (Supplementary Fig. 37).



New Supplementary Figure 37. SIM images of representative regions of LDs in HepG2 cells labeled with Plin2-mCherry, Plin5-GFP, **LDM**, and Cidec-GFP. (a) Representative images. (b) Quantitative analysis of LD-membrane contacts in HepG2 cells. $n = 10$. Data are shown as mean \pm SD (ns, not significant, **** $p < 0.0001$).

Comment 3: These points only require simple quantifications, not additional experiments, which the authors have already conducted extensively.

My intention is not to be overly critical or subjective but to ensure that the authors present tools that can genuinely advance research in this field.

The work done so far is indeed impressive, and I believe addressing these points will further strengthen the manuscript.

Response: We thank the reviewer for the positive and encouraging notes on our efforts to improve the manuscript.

REVIEWERS' COMMENTS

Reviewer #2 (Remarks to the Author):

The concerns from reviewers have been well addressed and the revised manuscript can be published.

Reviewer #3 (Remarks to the Author):

This referee's concerns have been addressed.